KEK layout

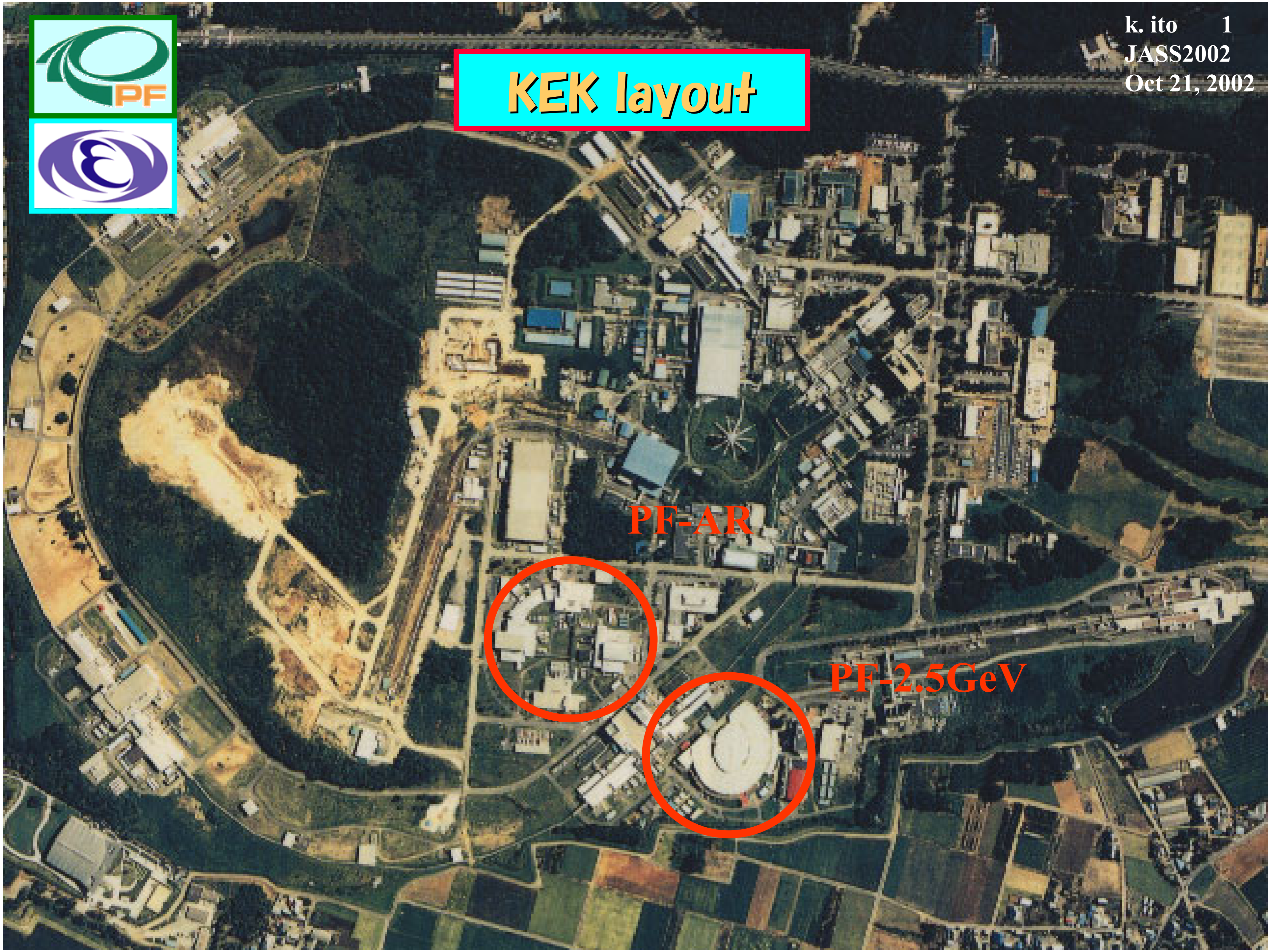

Layout of the Photon Factory

PF 2.5GeV Ring and Beam Lines

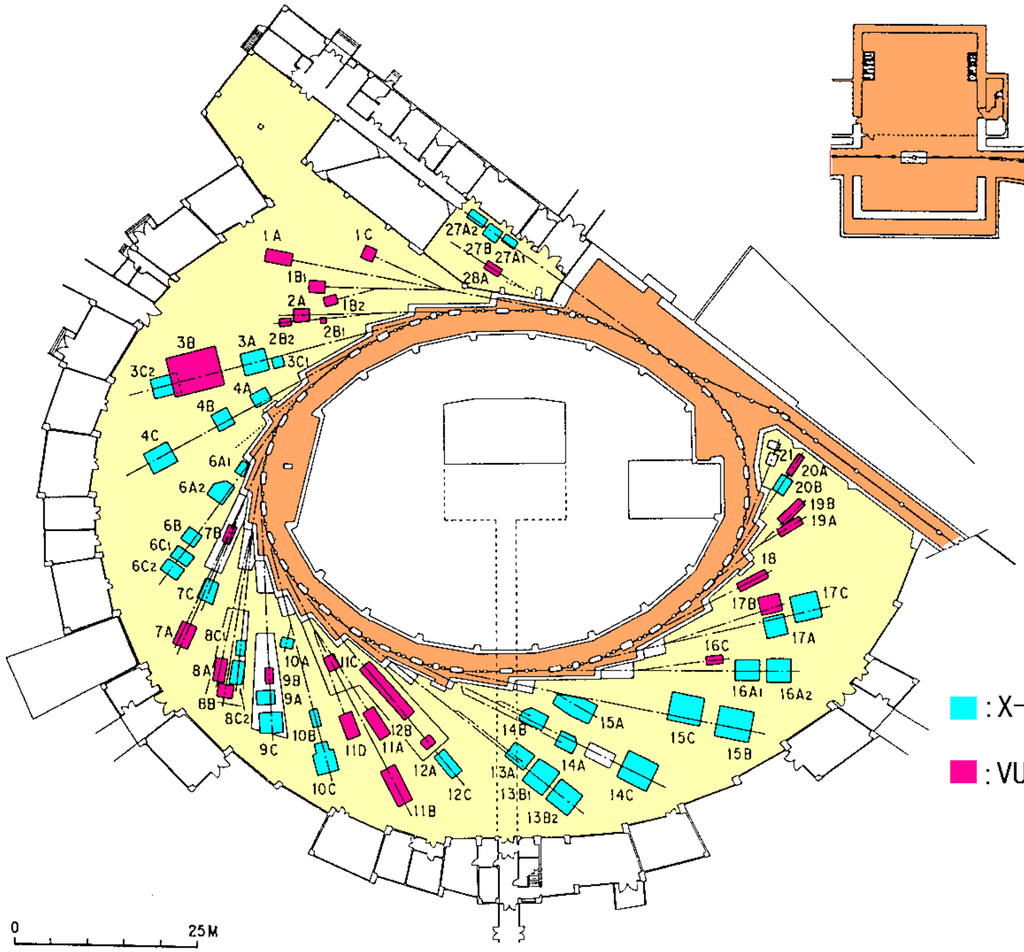

PF-AR(6.5GeV) Beam Lines

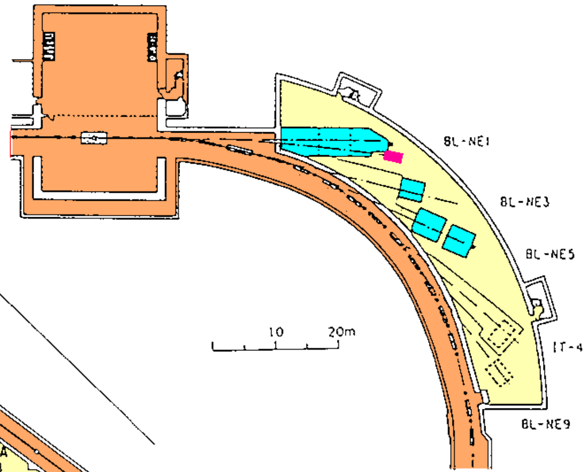

:X-ray beam lines

:VUV and soft X-ray beam lines

Synchrotron radiation beamlines in the vacuum ultraviolet and soft X-ray region

Kenji ITO e-mail: kenji.ito@kek.jp
Photon Factory, IMSS, KEK, Tsukuba, Ibaraki 305-0801, Japan

Introduction

Optical elements

- mirrors
  - geometrical shape
  - reflectivity
- grating
  - basic understanding
  - geometrical optics → ray tracing
  - varied-line spacing grating

Monochromators

- normal incidence type
- grazing incidence type

Summary

What is the role of beamlines for SR usage?

1) conducting SR from the storage ring to the experimental stations

2) shaping SR beam, spatially and energetically, to meet the experimental requirements

Definition of VUV and SX

VUV: vacuum ultraviolet

EUV: extreme ultraviolet

SX: soft X-ray

VUV-SX photons cannot propagate in the atmosphere!!!

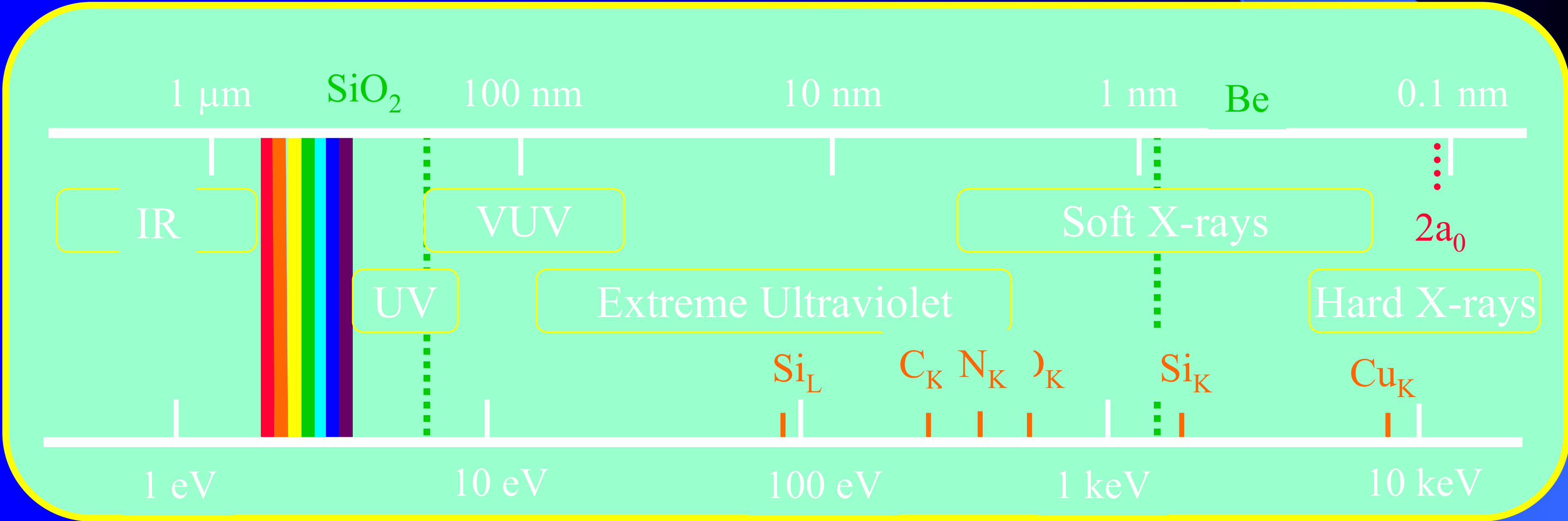

D. Attwood, "Soft X-rays and extreme ultraviolet radiation" (1999)

VUV-SX beamlines must be kept at ultra-high vacuum (UHV)

1) To facilitate the propagation of the VUV-SX photons

2) Not to disturb the storage ring
   no mechanically-rigid window is available!!!

3) To protect the optical elements from contamination,
   oil-free primary pumps are recommended!!!

Layout of a typical beamline

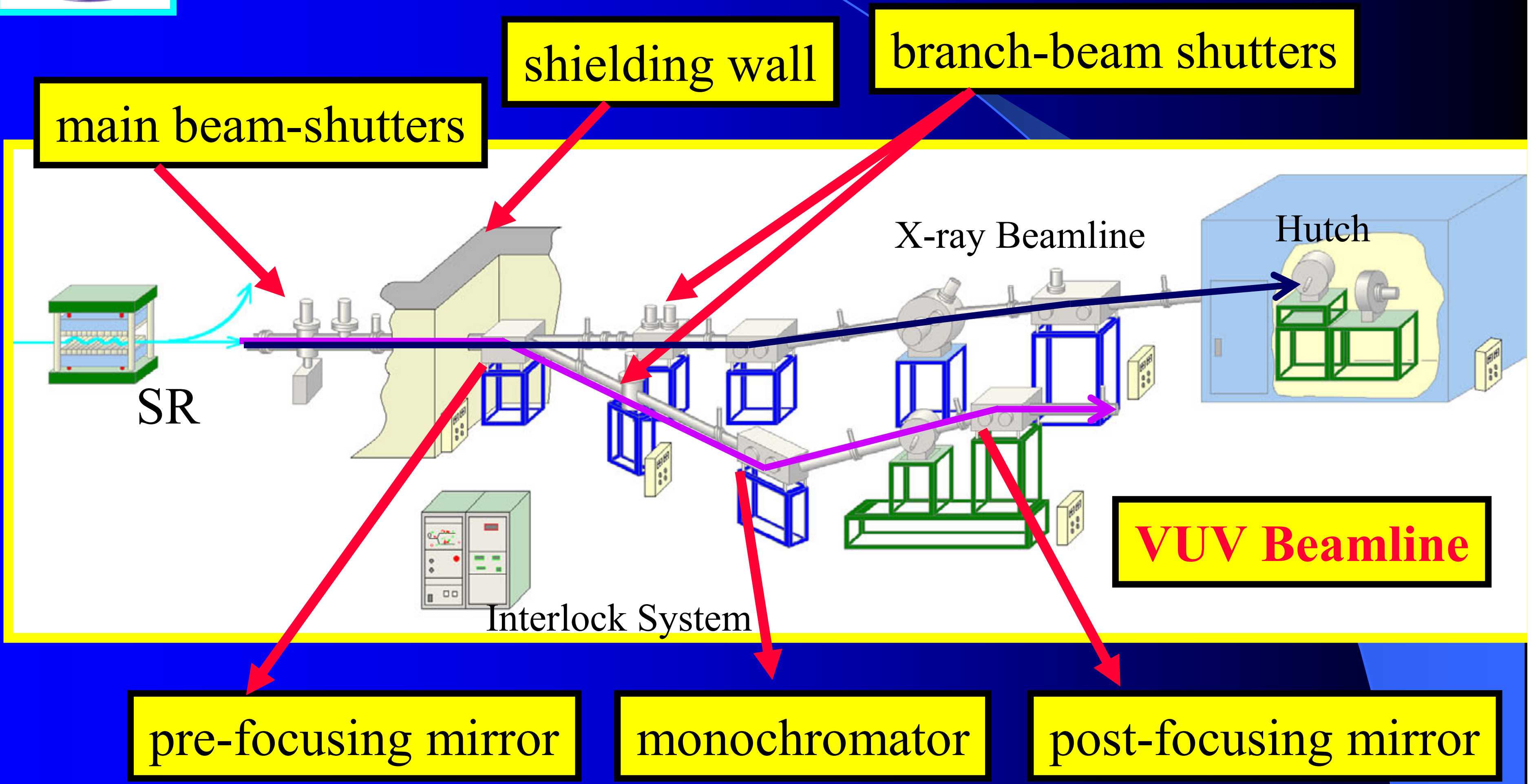

Construction of a VUV-SX beamline

What kinds of measurements are required?

Photon energy range
Photon flux
Beam size
Photon band width
Polarization
Purity
Coherence

Light source
- bending magnet
- undulator
- multipole wiggler

Beamline optics
- pre-focusing mirrors
- monochromator
- post-focusing mirrors

This procedure does not work for a multipurpose beamline.

Optical elements used in the VUV-SX beamlines

1) reflection mirrors as a focussing tool

2) diffraction gratings, zone plates, multi-layered mirrors, filters and crystals as dispersion tools

↓

monochromators as a beamline system

Mirrors for SR use

1) focusing of VUV-SX light by various shapes of mirror:
   sphere, cylinder, parabola, paraboloid, ellipse, ellipsoid, toroid, etc

2) for better reflectivity in the VUV-SX region:
   substrate: SiC, Si, SiO_2, metal, other glass
   coating materials: Au, Pt, Os,…

with modern technology:
- 1-m long mirrors available
- surface roughness < 0.5 nm in rms
- slope error < 1 μrad → beamspot size

Focusing mirrors of spherical shape

Astigmatism of spherical mirror

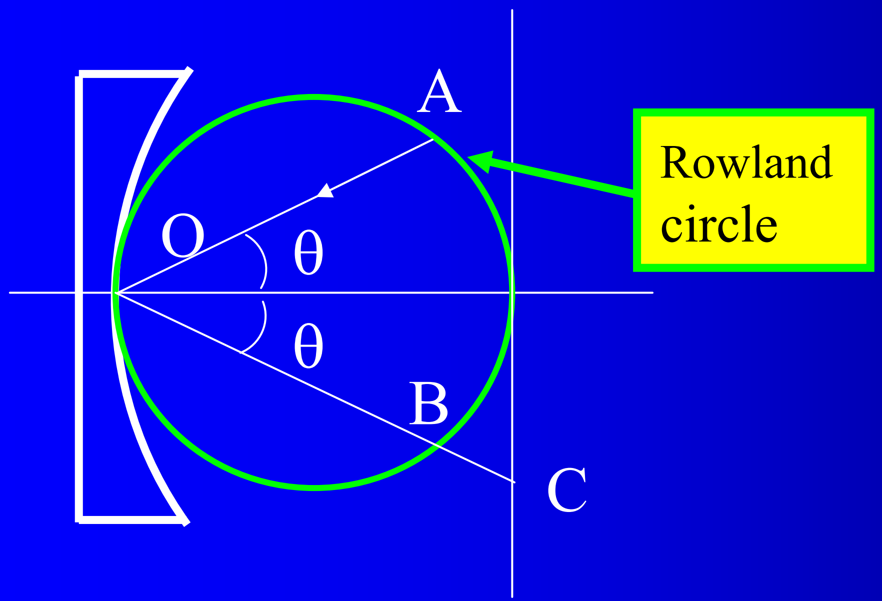

$AO = r \qquad OB = r_t \qquad OC = r_s$

$$\frac{1}{r} + \frac{1}{r_t} = \frac{2}{R\cos\theta}$$

$$\frac{1}{r} + \frac{1}{r_s} = \frac{2\cos\theta}{R}$$

Aberration of spherical mirror

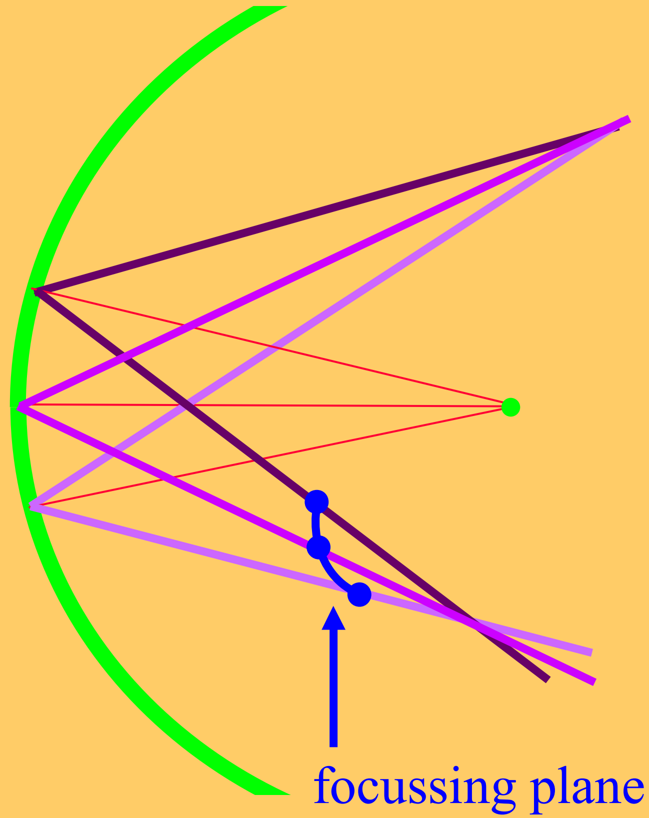

To avoid astigmatism: Focusing mirrors of toroidal shape

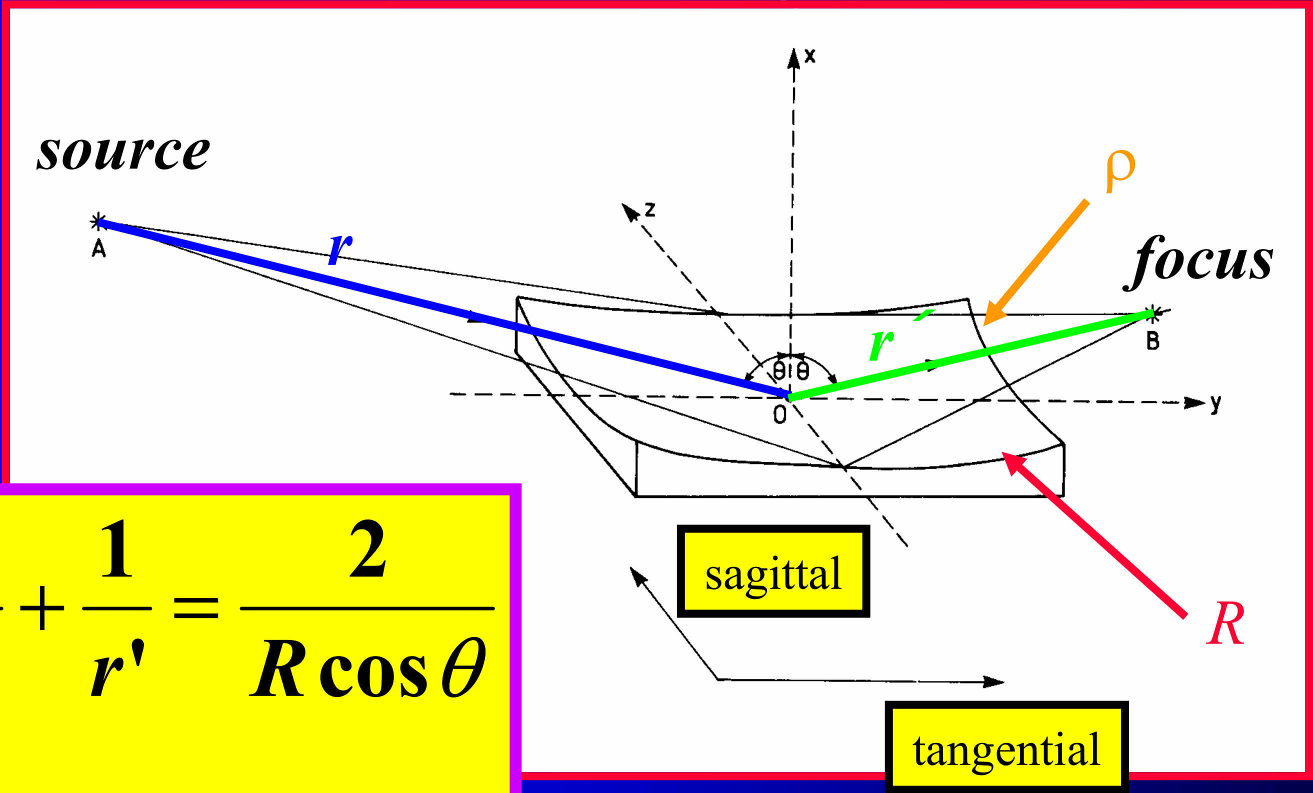

$$\frac{1}{r}+\frac{1}{r'}=\frac{2}{R\cos\theta}$$

$$\frac{1}{r}+\frac{1}{r'}=\frac{2\cos\theta}{\rho}$$

Parabolic mirrors to avoid aberration

In 2D focusing: paraboloidal

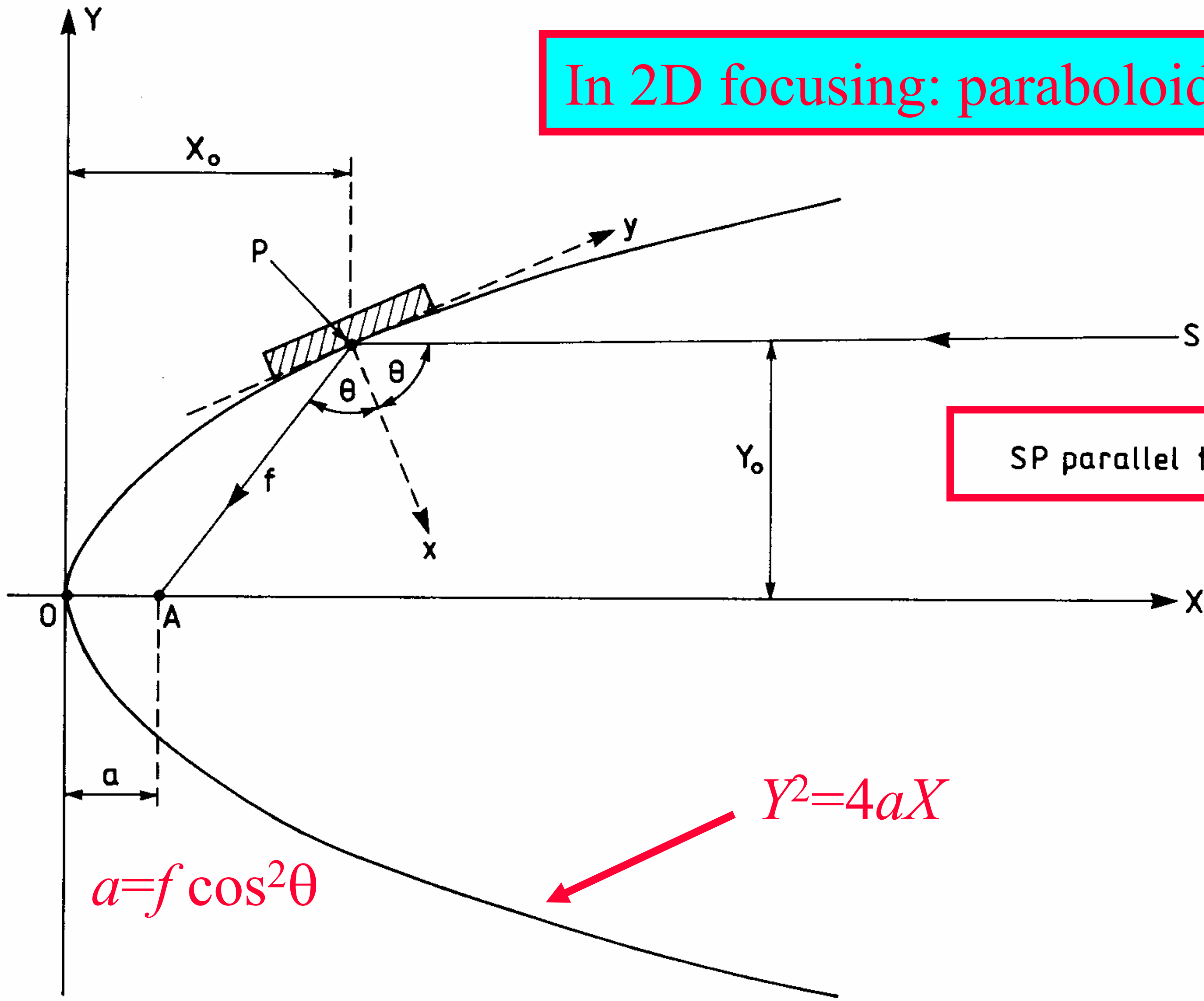

SP parallel to XO

$Y^2=4aX$

$a=f\cos^2\theta$

Elliptical mirrors to reduce aberration

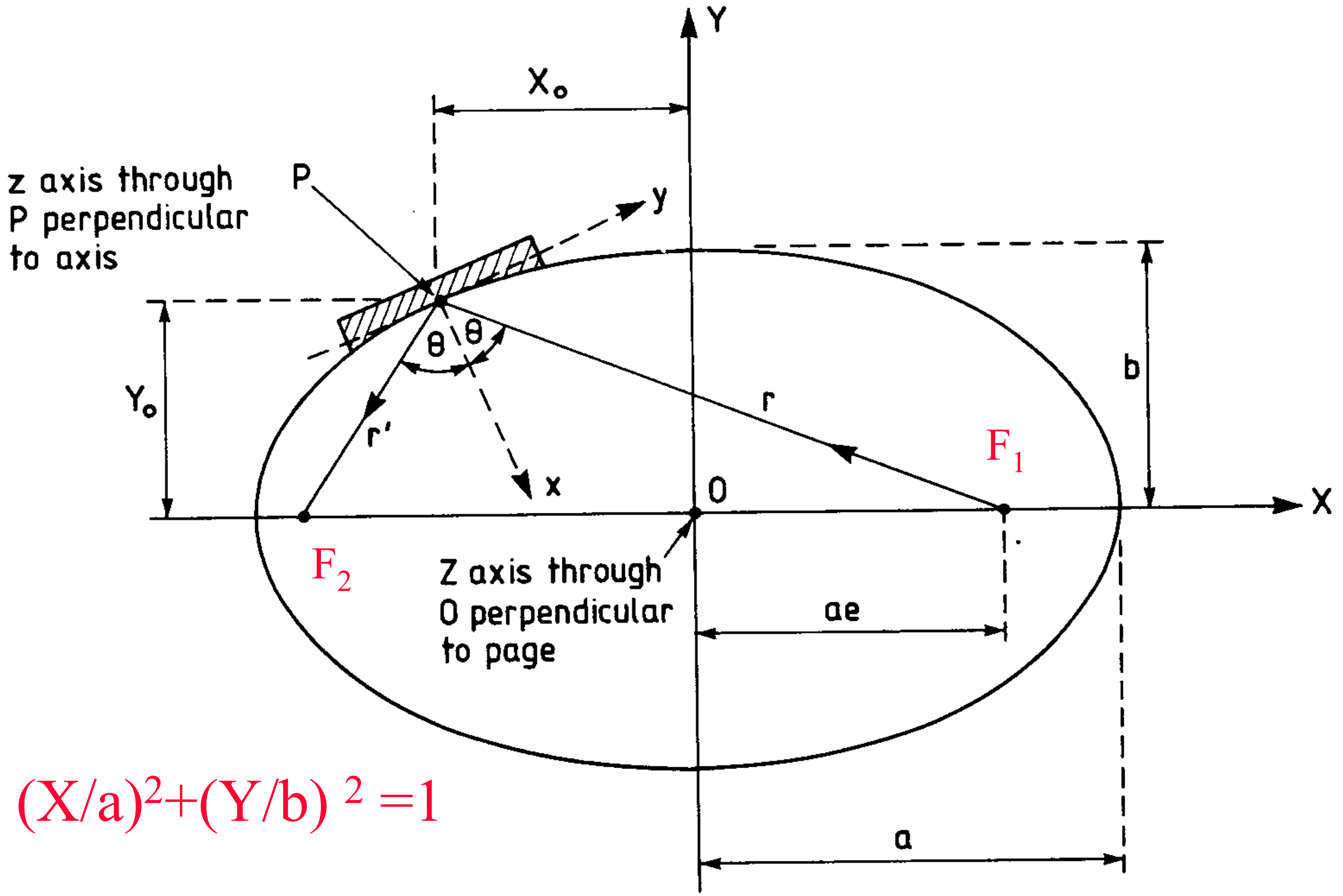

$$(X/a)^2+(Y/b)^2=1$$

For 2D focusing: ellipsoidal shape mirrors

Reflectivity of mirrors

$$R_s = \frac{a^2 + b^2 - 2s\cos\theta + \cos^2\theta}{a^2 + b^2 + 2s\cos\theta + \cos^2\theta}$$

$$R_p = R_s\left(\frac{a^2 + b^2 - 2a\sin\theta\tan\theta + \sin^2\theta\tan^2\theta}{a^2 + b^2 + 2a\sin\theta\tan\theta + \sin^2\theta\tan^2\theta}\right)$$

$$2a^2 = \left[\left(n^2 - k^2 - \sin^2\theta\right)^2 + 4n^2k^2\right]^{\frac{1}{2}} + \left(n^2 - k^2 - \sin^2\theta\right)$$

$$2b^2 = \left[\left(n^2 - k^2 - \sin^2\theta\right)^2 + 4n^2k^2\right]^{\frac{1}{2}} - \left(n^2 - k^2 - \sin^2\theta\right)$$

$R_s = R_p^2$ for 45°

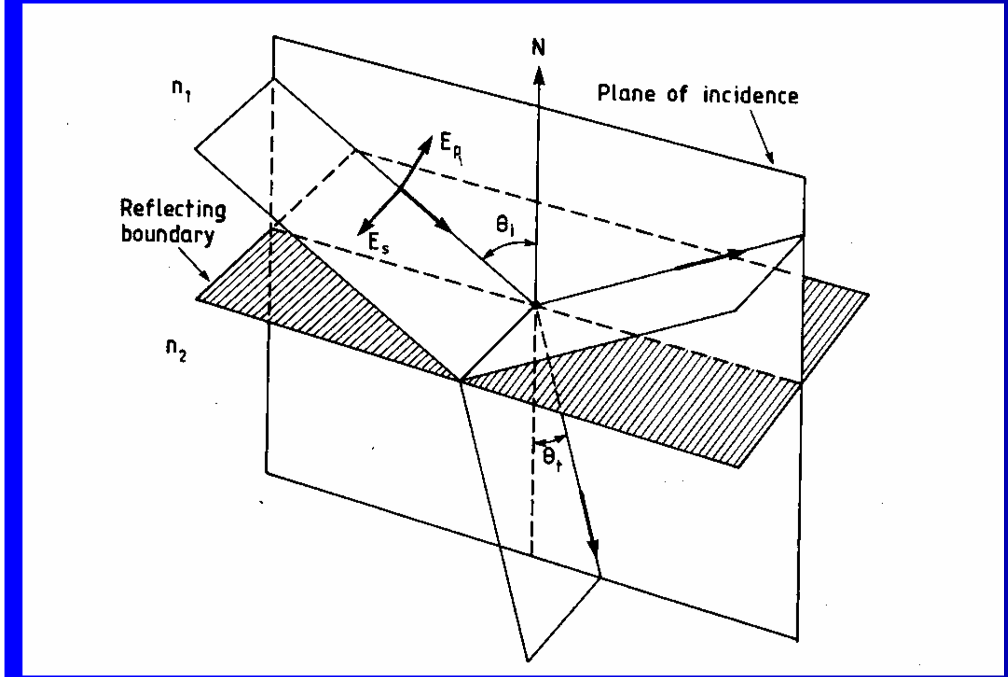

Complex refractive index
$\tilde{N} = n - ik$

↑

complex dielectric constant

↑

complex atomic scattering factor

Reflectivity of gold at 21.2 eV

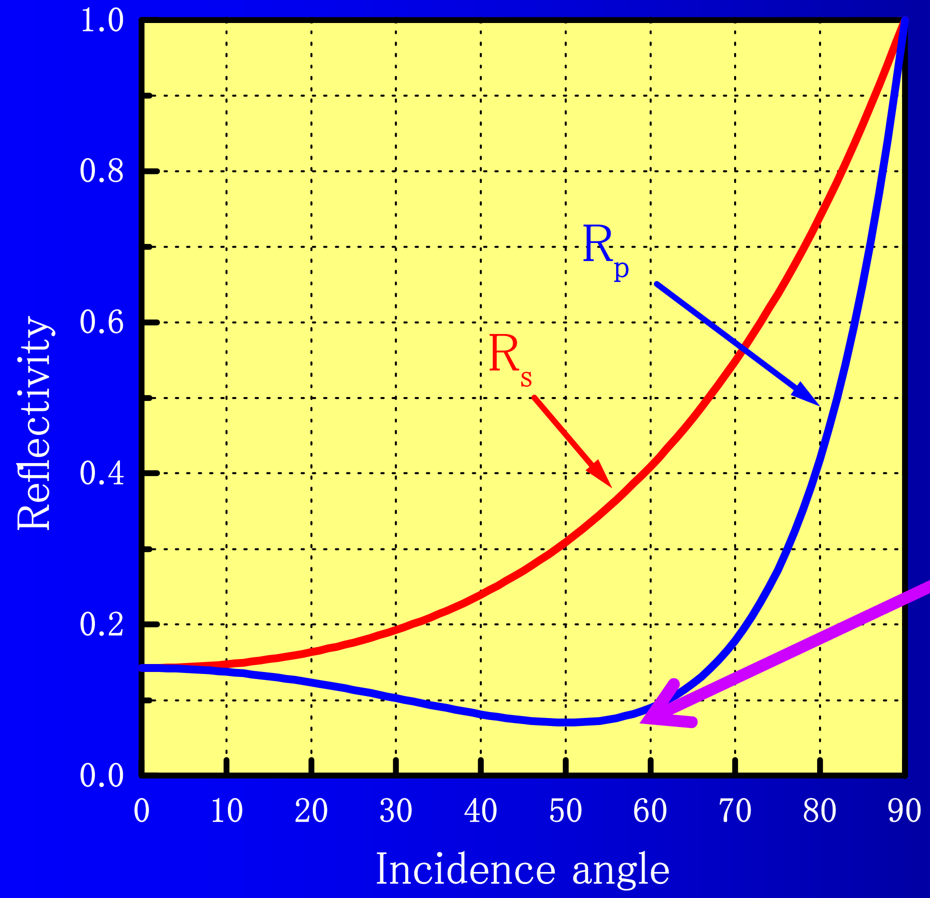

Brewster angle

R_p=0 for dielectric material

Atomic scattering factor for Au

$$\tilde{F} = f_1 + if_2$$

$$f_1 = Z + C\int_0^{\infty} \frac{\varepsilon^2 \mu_a(\varepsilon) d\varepsilon}{E^2 - \varepsilon^2}$$

$$f_2 = (\pi / 2) C E \mu_a(\varepsilon)$$

↓

$$K = 1 - \alpha - i\gamma$$

$$\alpha = D f_1$$

$$\gamma = D f_2$$

↓

$$\tilde{N} = n - ik$$

$$\tilde{N}^2 = \tilde{K}$$

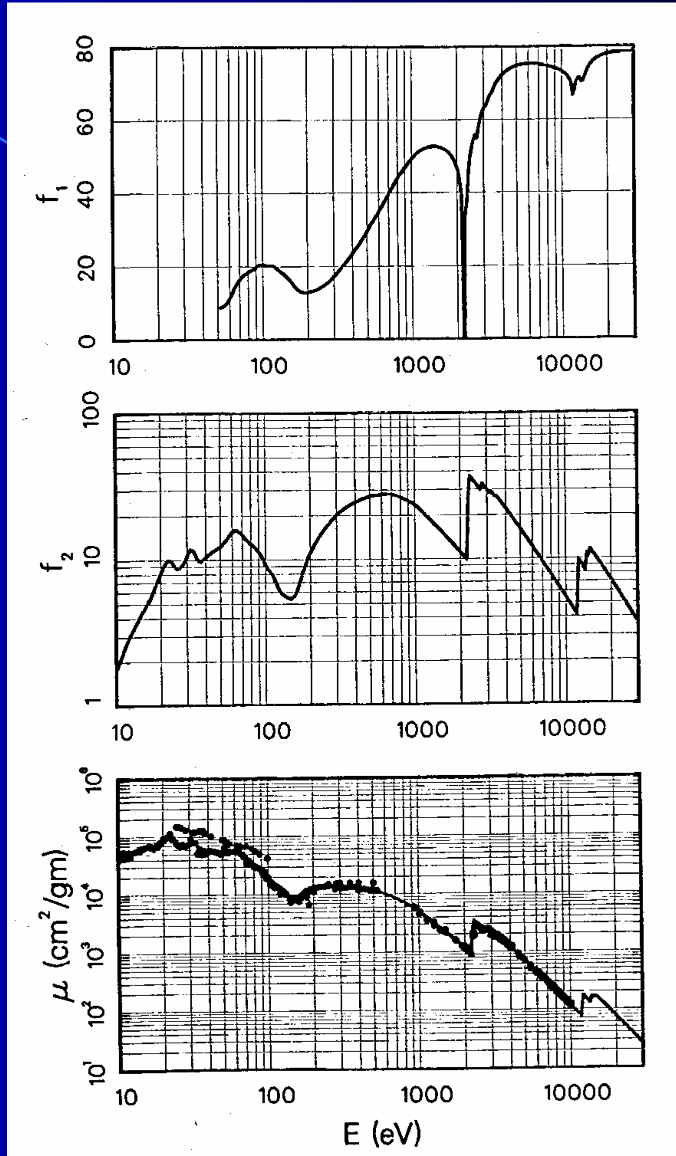

Henke, Gullikson and Davis, Atomic Data and Neclear Data Tables, **54**, 181 (1993)

Reflectivity of gold for s-polarization

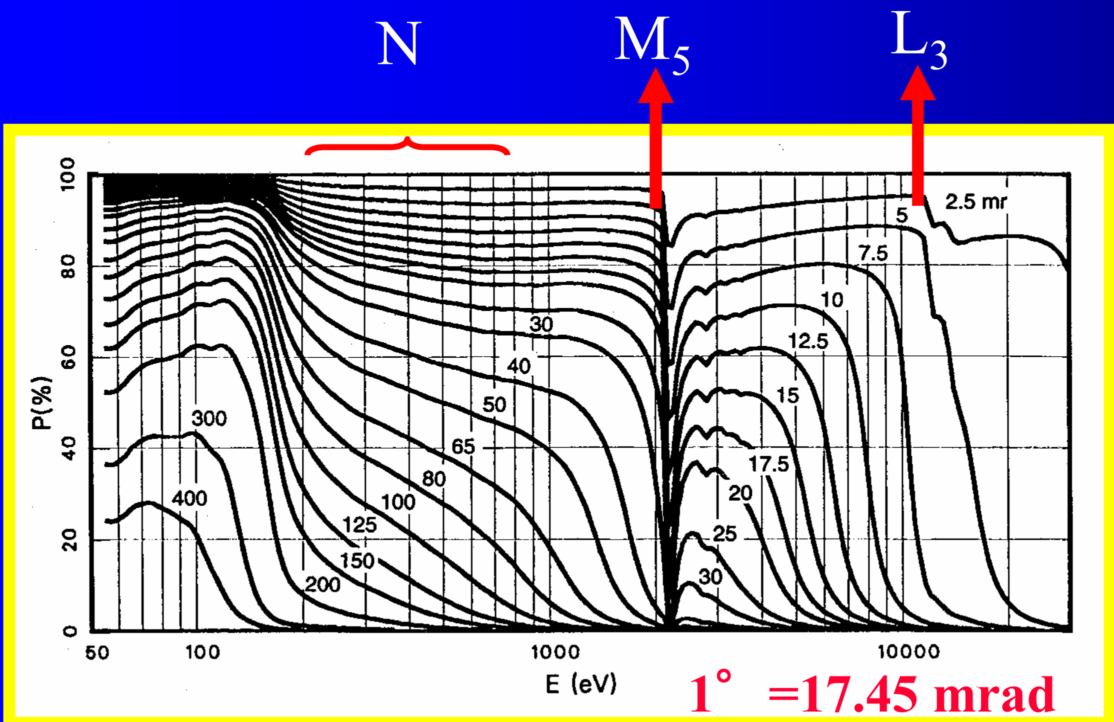

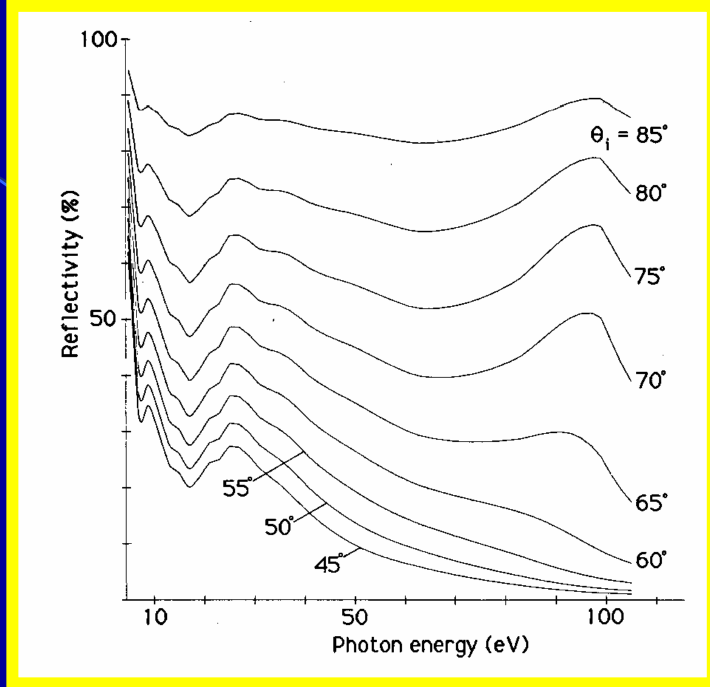

Mirrors can play the role of low pass filters.

Henke et al., Atomic and Nuclea Data Tables, **54**, 181 (1993)

Surface roughness reduces the reflectivity

$R = R_0 \exp[-(4\pi\sigma \sin\phi/\lambda)^2]$

σ : micro surface roughness in rms <0.5 nm

ϕ : glancing angle

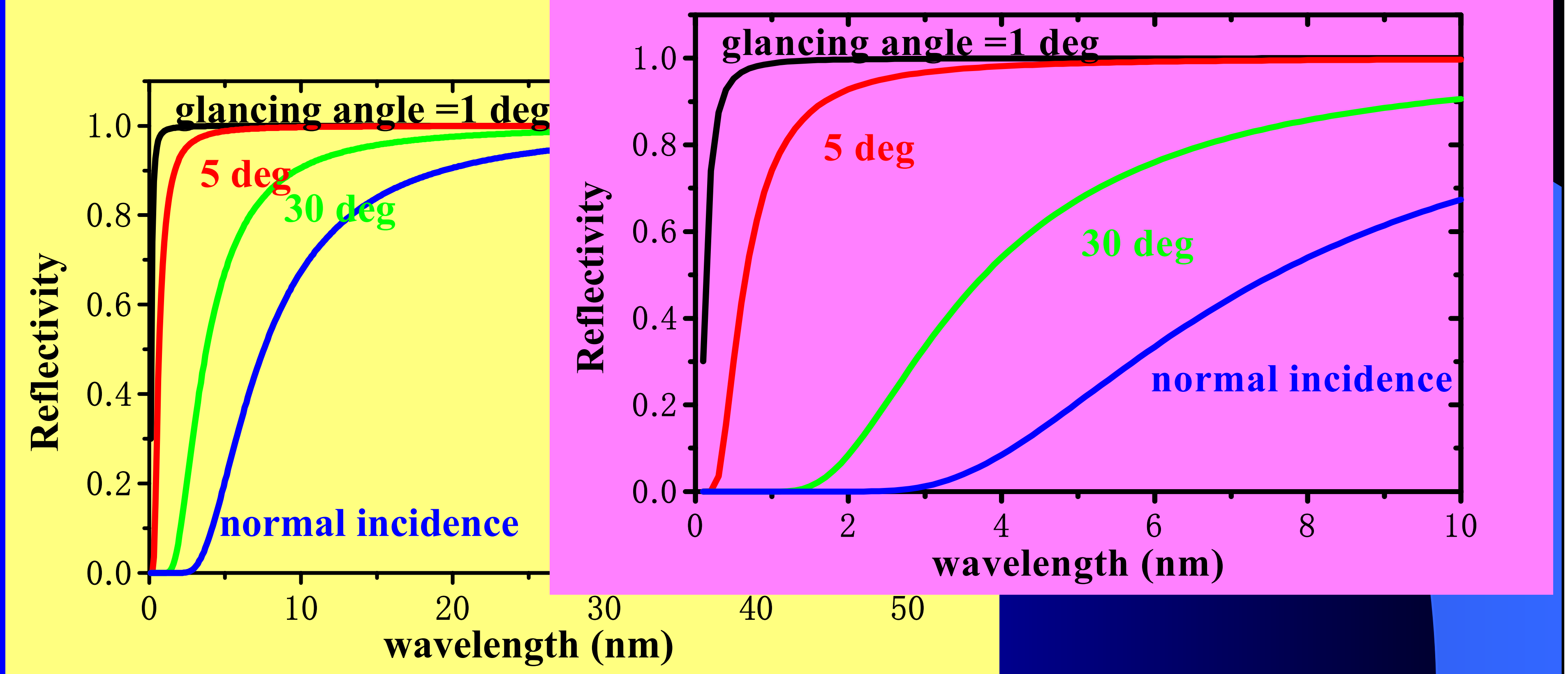

Gratings as dispersion elements

Diffraction grating
Zone plate
Multi-layered mirror
Filters
Crystals

1) Introduction
2) Efficiency
3) Geometrical optics → ray tracing
4) Varied-line spacing grating

Equation for diffraction grating

$$I = a^2 \frac{\sin^2[(\pi b/\lambda)(\sin\alpha + \sin\beta)]}{(\pi b/\lambda)^2(\sin\alpha + \sin\beta)^2} \frac{\sin^2(N\Delta/2)}{\sin^2(\Delta/2)}$$

a: amplitude of incident light

$$\Delta = \frac{2\pi d}{\lambda}(\sin\alpha + \sin\beta)$$

I has maximal values for $\Delta = 2m\pi$.

$$\sin\alpha + \sin\beta = \frac{m\lambda}{d}$$

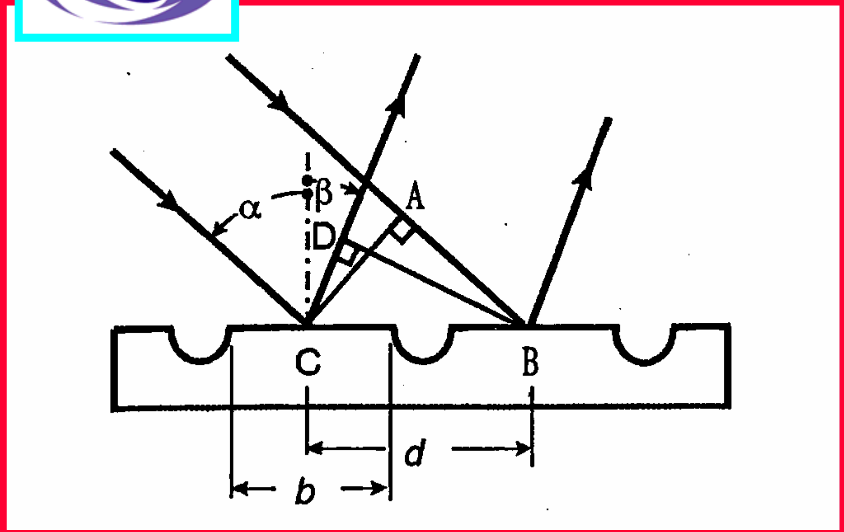

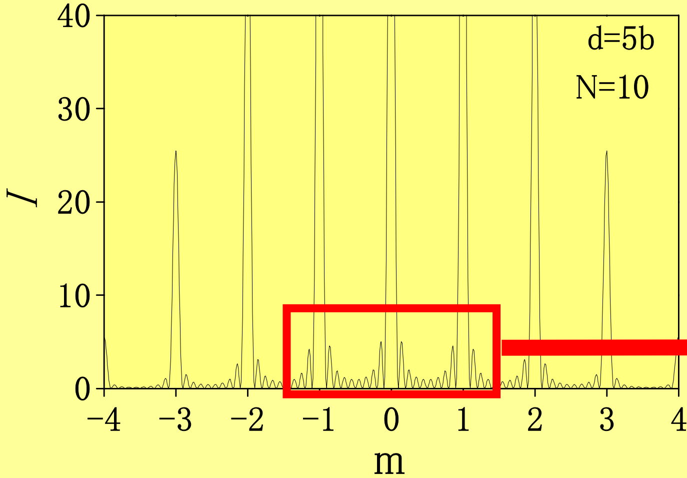

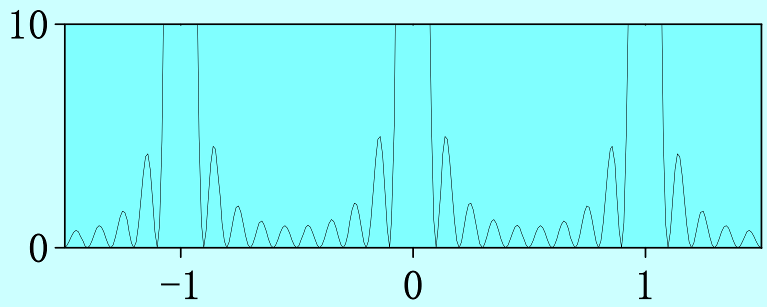

Dispersion of diffraction grating

$$\sin\alpha + \sin\beta = \frac{m\lambda}{d}$$

Angular dispersion: $\left(\frac{\partial\lambda}{\partial\beta}\right)_\alpha = \frac{d\cos\beta}{m}$

Reciprocal linear dispersion: $\left(\frac{\partial\lambda}{\partial q}\right)_\alpha = \frac{10^6 d[mm]\cos\beta\cos\phi}{mr'[mm]} nm/mm$

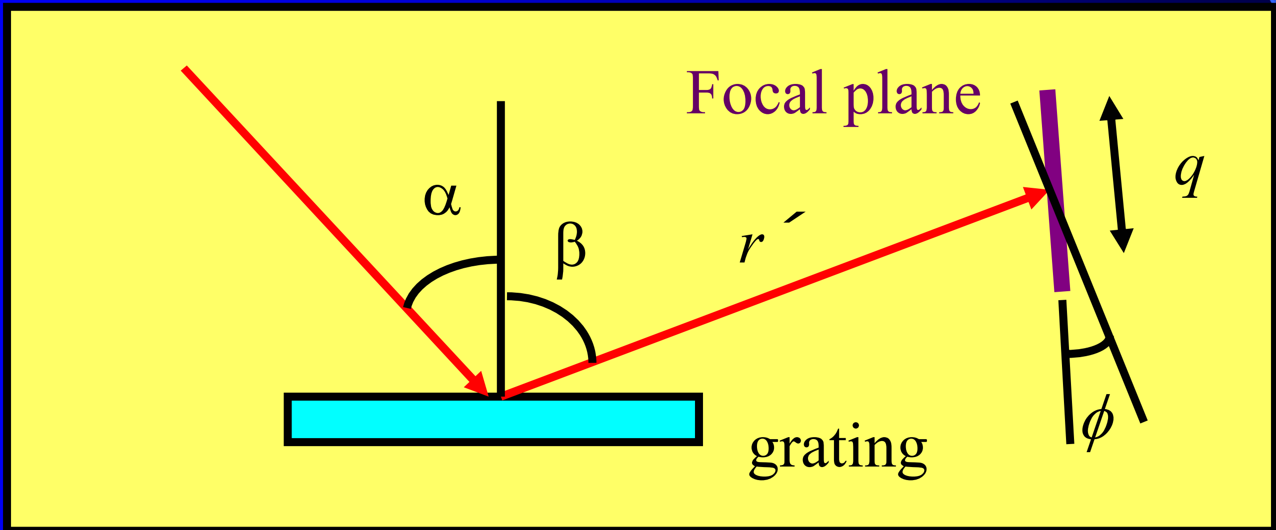

Diffraction efficiency

$$\sin\alpha + \sin\beta = \frac{m\lambda}{d}$$

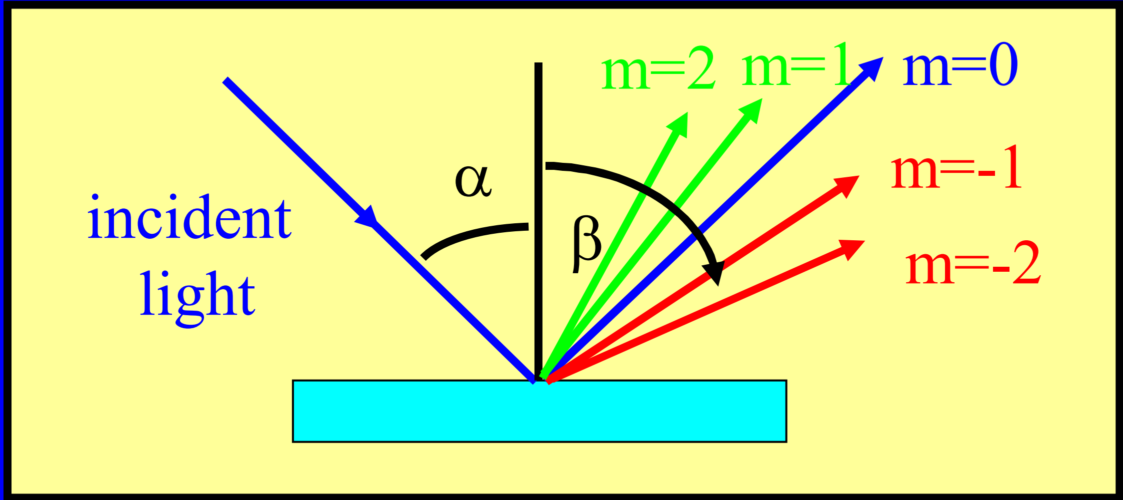

m>0 positive order
inside order
m<0 negative order
outside order

Diffraction efficiency can be calculated by the scalar theory for $\lambda/d \ll 1$. Rigorous numerical calculations based on Maxwell equations gives solutions with much better precision.
Note that the efficiency strongly depends on the polarization of incident radiation.

Blazed grating

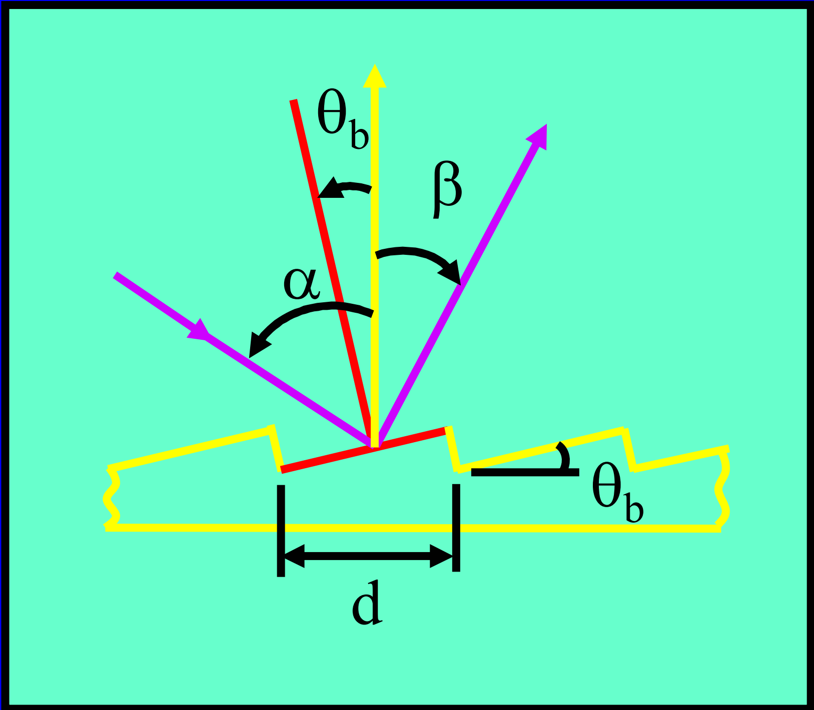

Maximal efficiency can be achieved at

$$\alpha-\theta_b=\theta_b-\beta.$$

$$m\lambda_{bK}=2d\sin\theta_b\cos K$$

where blazed wavelength is λ_{bK} and deviation angle is $2K=\alpha-\beta$.

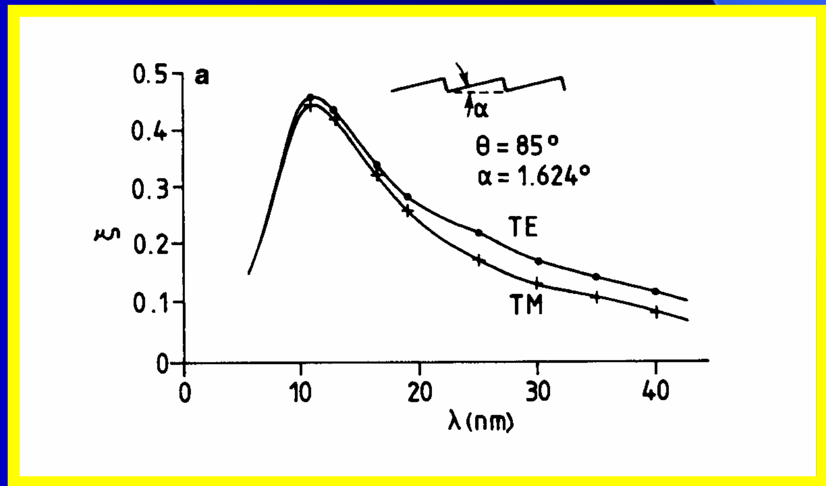

Calculated by M. Neviere

Laminar grating(1)

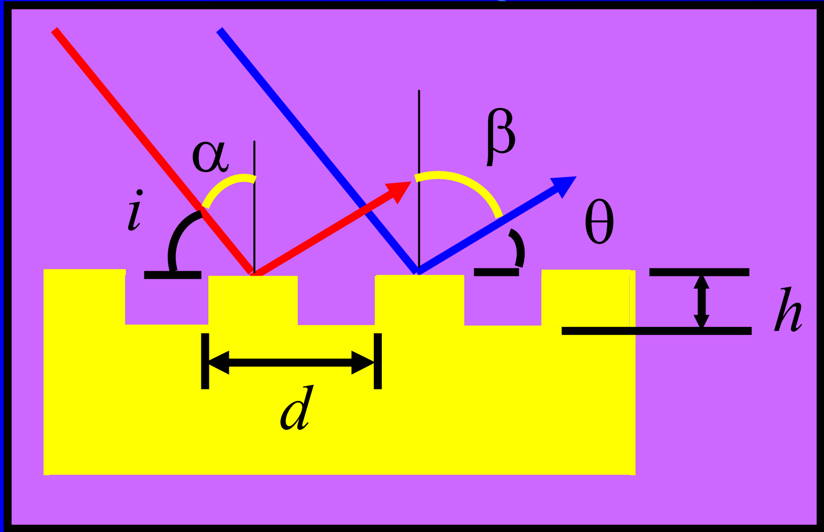

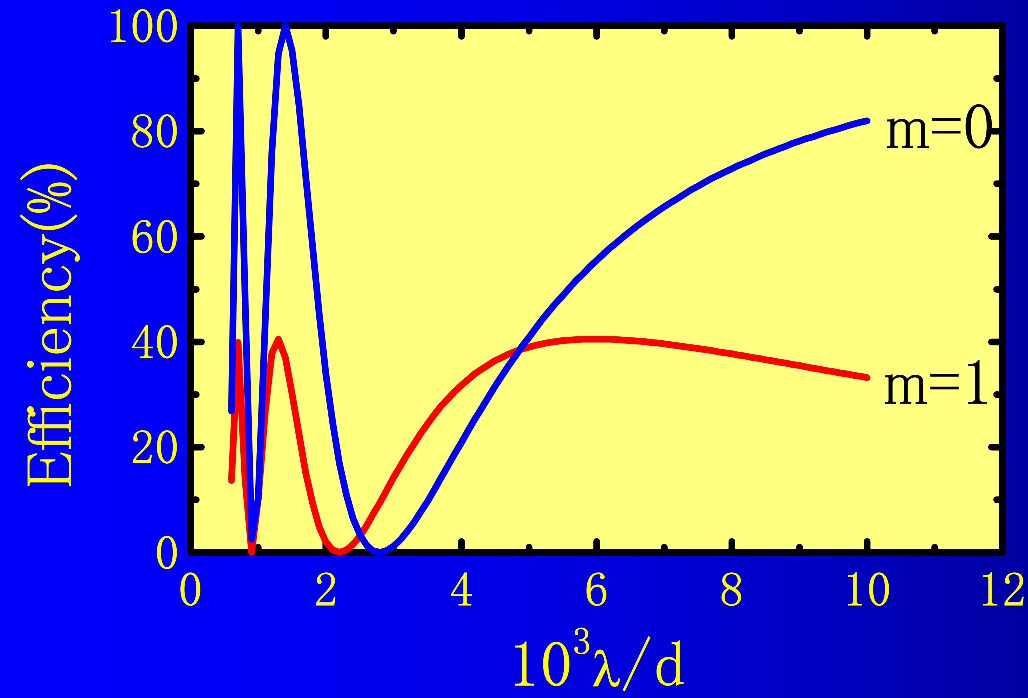

Grating equation

$\sin\alpha + \sin\beta = m\lambda/d$

Efficiency

$E_0 = 100\cos^2(\delta/2)$

$E_m = (400/m^2\pi^2)\sin^2(\delta/2)$

$\delta = (2\pi/\lambda)h(\sin i + \sin\theta)$

Primary maximum

$\lambda/d = [2m\cos i + (\sin\theta)/p]$

$\times (p^2/4 + m^2)$

where $P = h/d$

Laminar grating(2)

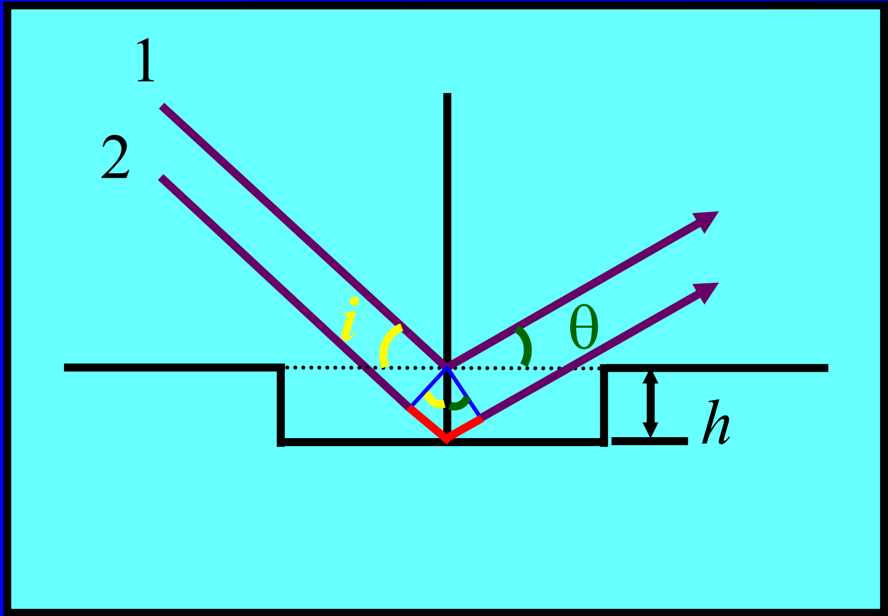

When the path difference between 1 and 2 is equal to λ/2, destructive interference occurs.

$h(\sin i+\sin\theta)= \lambda/2$

normal incidence: $\lambda=4h$

grazing incidence: $\lambda=2h(i+\theta)$

Suppression of 2nd order!!!

Geometrical optics of diffraction gratings(1)

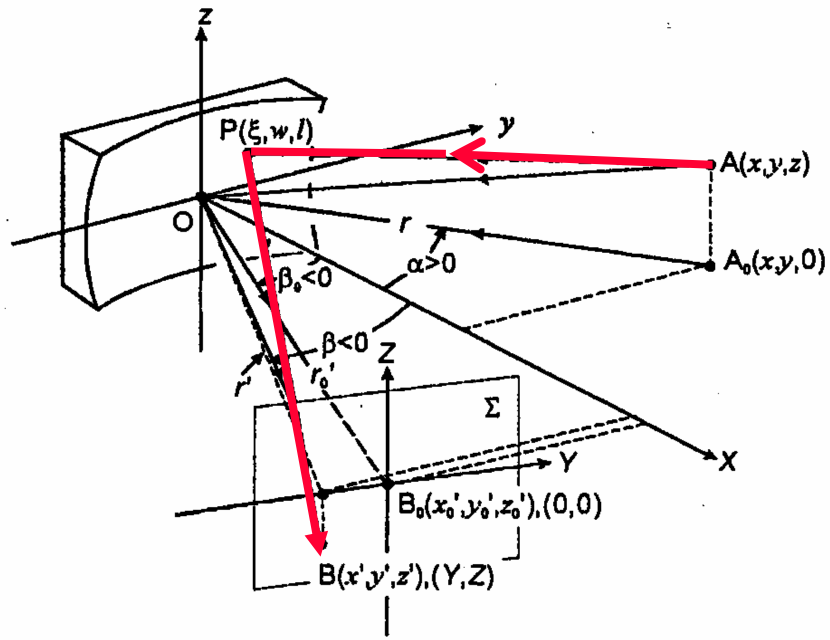

Fermat's principle: the pathlength of an actual ray traveling from a point A to a point B takes an extremal or stationary value.

$\delta F=0$, where F is the pathlength from A to B. F: light path function

The red ray meets the grating at a point P(ξ,w,l) on the nth groove, the zeroth groove being assumed to pass through O. Two rays diffracted from the zeroth and nth grooves are reinforced when their path difference is equal to $nm\lambda$.

Light path function
F=AP+PB+$nm\lambda$

$$AP = \sqrt{(\xi - x)^2 + (w - y)^2 + (l - z)^2}$$

$$PB = \sqrt{(x'-\xi)^2 + (y'-w)^2 + (z'-l)^2}$$

Geometrical optics of diffraction gratings(2)

Expansion of *F* for *z*=0 and *n*=1/*d*

$$F = F_{00} + F_{10} w + \frac{1}{2} F_{20} w^2 + \frac{1}{2} F_{02} l^2 + \frac{1}{2} F_{30} w^3 + \frac{1}{2} F_{12} wl^2$$
$$+ \frac{1}{8} F_{40} w^4 + \frac{1}{4} F_{22} w^2 l^2 + \frac{1}{8} F_{04} l^4 + \ldots..$$

F_{40}: spherical aberration; F_{04}: astigmatism

$$F_{00} = r + r_0'$$

$$F_{10} = -\sin\alpha - \sin\beta_0 + \frac{m\lambda}{d}$$ grating equation

$$F_{20} = \frac{\cos^2\alpha}{r} - \frac{\cos\alpha}{R} + \frac{\cos^2\beta_0}{r_0'} - \frac{\cos\beta_0}{R}$$ defocus in y-direction

$$F_{02} = \frac{1}{r} - \frac{\cos\alpha}{R} + \frac{1}{r_0'} - \frac{\cos\beta_0}{R}$$ defocus in z-direction

$$F_{30} = \frac{\sin\alpha}{r}\left(\frac{\cos^2\alpha}{r} - \frac{\cos\alpha}{R}\right) + \frac{\sin\beta_0}{r_0'}\left(\frac{\cos^2\beta_0}{r_0'} - \frac{\cos\beta_0}{R}\right)$$ comma

Geometrical optics of diffraction gratings(3)

Apply Fermat's principle to F

$$\delta F = \frac{\partial F}{\partial w}\delta w + \frac{\partial F}{\partial l}\delta l = 0 \Rightarrow \frac{\partial F}{\partial w} = 0, \quad \frac{\partial F}{\partial l} = 0 \Rightarrow \frac{\partial F_{ij}}{\partial w} = 0, \quad \frac{\partial F_{ij}}{\partial l} = 0$$

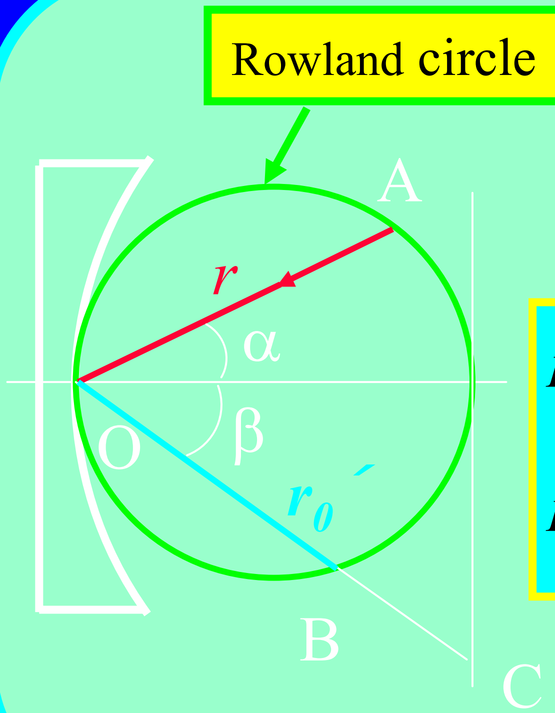

Roland mount

$r = R\cos\alpha \quad r_0' = R\cos\beta_0$

$$F_{20} = \frac{\cos^2\alpha}{r} - \frac{\cos\alpha}{R} + \frac{\cos^2\beta_0}{r_0'} - \frac{\cos\beta_0}{R}$$

$$F_{30} = \frac{\sin\alpha}{r}\left(\frac{\cos^2\alpha}{r} - \frac{\cos\alpha}{R}\right) + \frac{\sin\beta_0}{r_0'}\left(\frac{\cos^2\beta_0}{r_0'} - \frac{\cos\beta_0}{R}\right)$$

$F_{20}=F_{30}=0$

Geometrical optics of diffraction gratings(4)

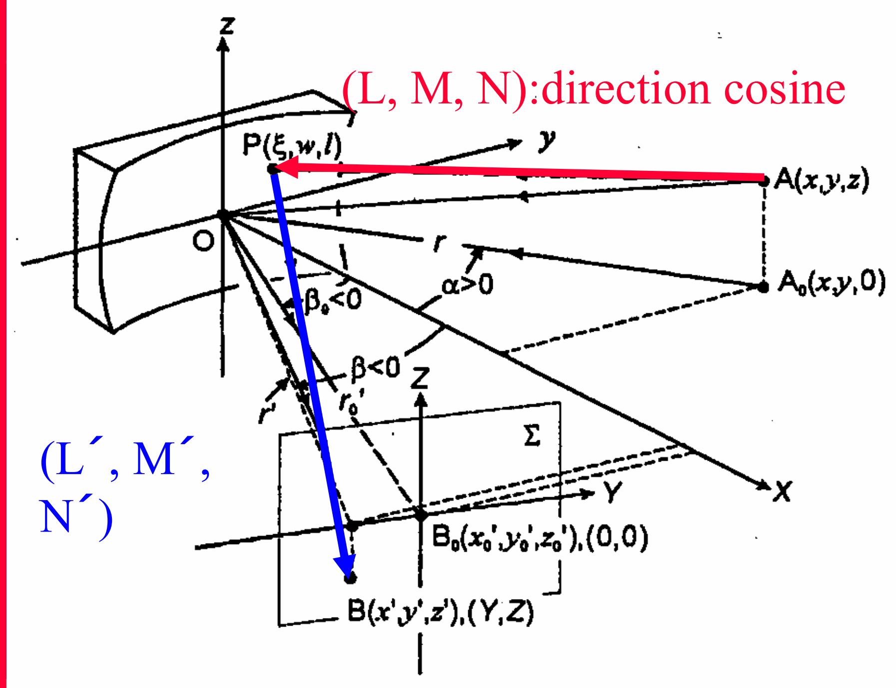

Ray-tracing

$$F = AP + PB + nm\lambda$$

$$\frac{\partial F}{\partial w} = (L - L')\frac{\partial \xi}{\partial w} + (M - M') + m\lambda\frac{\partial n}{\partial w} = 0$$

$$\frac{\partial F}{\partial l} = (L - L')\frac{\partial \xi}{\partial l} + (N - N') + m\lambda\frac{\partial n}{\partial l} = 0$$

$$L' = L + T$$

$$M' = M + m\lambda\frac{\partial n}{\partial w} - T\frac{\partial \xi}{\partial w}$$

$$N' = N + m\lambda\frac{\partial n}{\partial l} - T\frac{\partial \xi}{\partial l}$$

$$T = \frac{1}{e}\left(p + \sqrt{p^2 - eq}\right)$$

$$e = 1 + \left(\frac{\partial \xi}{\partial w}\right)^2 + \left(\frac{\partial \xi}{\partial l}\right)^2$$

$$p = -L + \left(M + m\lambda\frac{\partial n}{\partial w}\right)\frac{\partial \xi}{\partial w} + \left(N + m\lambda\frac{\partial n}{\partial l}\right)\frac{\partial \xi}{\partial l}$$

$$q = 2m\lambda\left(M\frac{\partial n}{\partial w} + N\frac{\partial n}{\partial l}\right) + (m\lambda)^2\left[\left(\frac{\partial n}{\partial w}\right)^2 + \left(\frac{\partial n}{\partial l}\right)^2\right]$$

Geometrical optics of diffraction gratings(5)

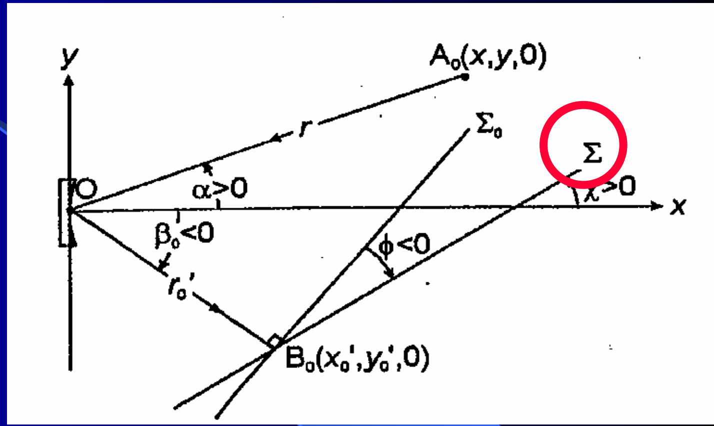

Equation of image plane:

$$x'\cos(\beta_0+\phi)+y'\sin(\beta_0+\phi)=r_0'\cos\phi$$

where

$$x'=\xi+L'd \qquad y'=w+M'd \qquad z'=l+N'd$$

$$d=\frac{r_0'\cos\phi-\xi\cos(\beta_0+\phi)-w\sin(\beta_0+\phi)}{L'\cos(\beta_0+\phi)+M'\sin(\beta_0+\phi)}$$

YZ-coordinate on Σ-plane

$$Y=(y'-r_0'\sin\beta_0)\sec(\beta_0+\phi)$$

$$Z=z'$$

$$Y=r_0'\sec\beta_0\sec\phi\times\left[wf_{100}+w^2f_{200}+l^2f_{020}+lzf_{011}+z^2f_{002}+w^3f_{300}+wl^2f_{120}+wlzf_{111}+wz^2f_{102}+O\left(w^4/R^3\right)\right]$$

$$Y=r_0'\left[zg_{001}+lg_{010}+wlg_{110}+wzg_{101}+w^2lg_{210}+w^2zg_{201}+l^3g_{030}+l^2zg_{021}+lz^2f_{012}+z^3f_{003}+O\left(w^4/R^3\right)\right]$$

Geometrical optics of diffraction gratings(6)

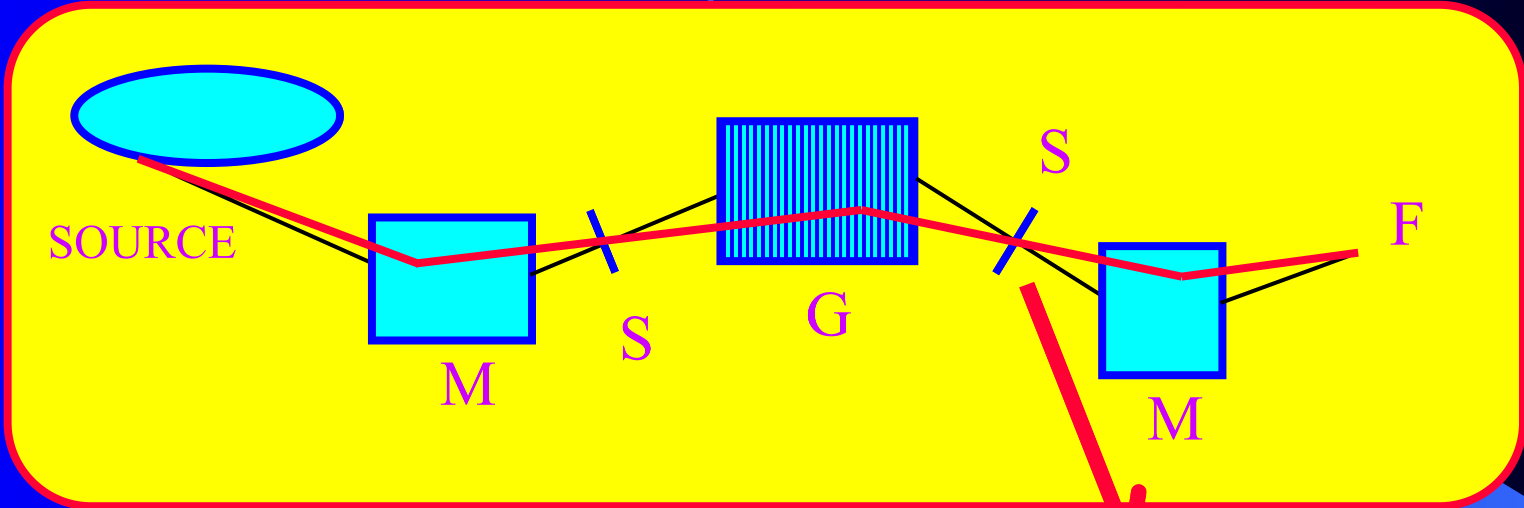

By ray-tracing, it is possible to see

1) how the beam is focused on the slits and at F,
2) how it spreads on the grating,
3) the geometrical through-put.

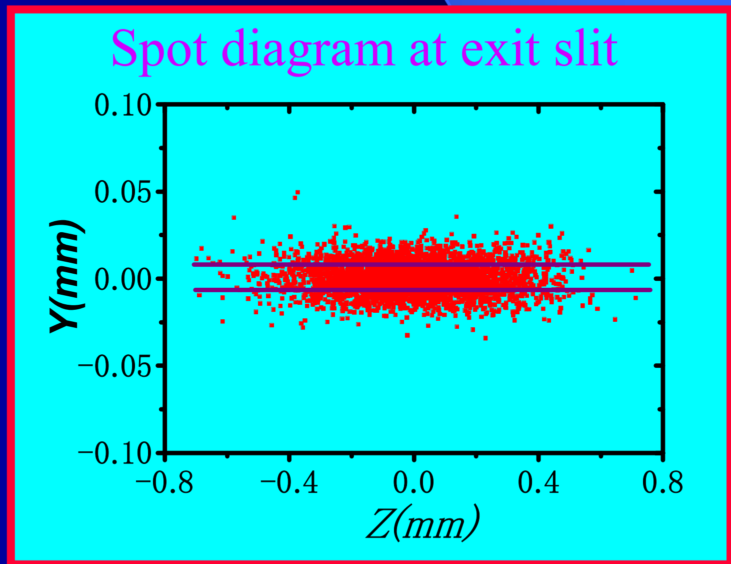

Geometrical optics of diffraction gratings(7)

Analytical expression for spot diagrams

$$Y = r_0' \sec\beta_0 \sec\phi \times \Big[wf_{100} + w^2 f_{200} + l^2 f_{020} + lzf_{011} + z^2 f_{002} + w^3 f_{300} + wl^2 f_{120} + wlzf_{111} + wz^2 f_{102} + O\left(\frac{w^4}{R^3}\right) \Big]$$

$$Z = r_0' \Big[zg_{001} + \lg_{010} + w\lg_{110} + wzg_{101} + w^2\lg_{210} + w^2 zg_{201} + l^3 g_{030} + l^2 zg_{021} + lz^2 f_{012} + z^3 f_{003} + O\left(\frac{w^4}{R^3}\right) \Big]$$

Analytical merit function: ***Q***

$$Q = \sum_i Q(\lambda_i)$$

$$= \sum_i \left[\frac{1}{WLH} \iiint (Y - \overline{Y})^2 \, dwdldz + \frac{\mu}{WLH} \iiint Z^2 \, dwdldz \right]$$

Optimization of design parameters so as to minimize ***Q***, where μ is a weight function. Triple integrals have to be done over the grating surface. Note that ***Y*** and ***Z*** are dependent on λ_i (i=1, 2, …N).

Masui and Namioka, JOSA, **16**, 2253 (1999)

Geometrical optics of diffraction gratings(8)

Hybrid design method : Koike and Namioka, JESRP, **80**, 303 (1996)

$$Y_n(w_n, l_n, z_n) = \sum_n f_{ijk} w_n^i l_n^j z_n^k$$

$$Z_n(w_n, l_n, z_n) = \sum_n g_{ijk} w_n^i l_n^j z_n^k$$

Ray-tracing of 18 rays determines f_{ijk}'s and g_{ijk}'s by solving simultaneous equations.
Optimization process using the merit function in the same manner as before.

Ray-tracing program is available at http://www.xraylith.wisc.edu/shadow/shadow.html

Varied line spacing gratings (1)

Groove function

$$n(w,l)\sigma = w + \Gamma\left[\frac{1}{2}\left(n_{20}w^2 + n_{02}l^2 + n_{30}w^3 + n_{12}wl^2\right) + \frac{1}{8}\left(n_{40}w^4 + 2n_{22}w^2l^2 + n_{04}l^4\right) + \ldots\right]$$

Effective grating constant

$$\sigma \equiv 1 \Big/ \left[\frac{\partial n(w,l)}{\partial w}\right]_{w=l=0}$$

Γ=**1** for mechanically ruled grating

$\Gamma=\sigma/\lambda_0$ for holographic grating

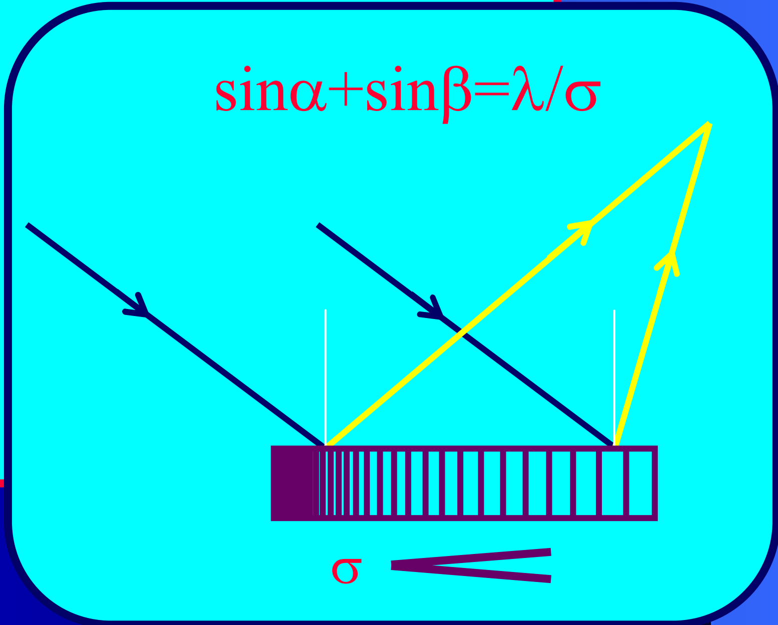

Varied line spacing gratings (2)

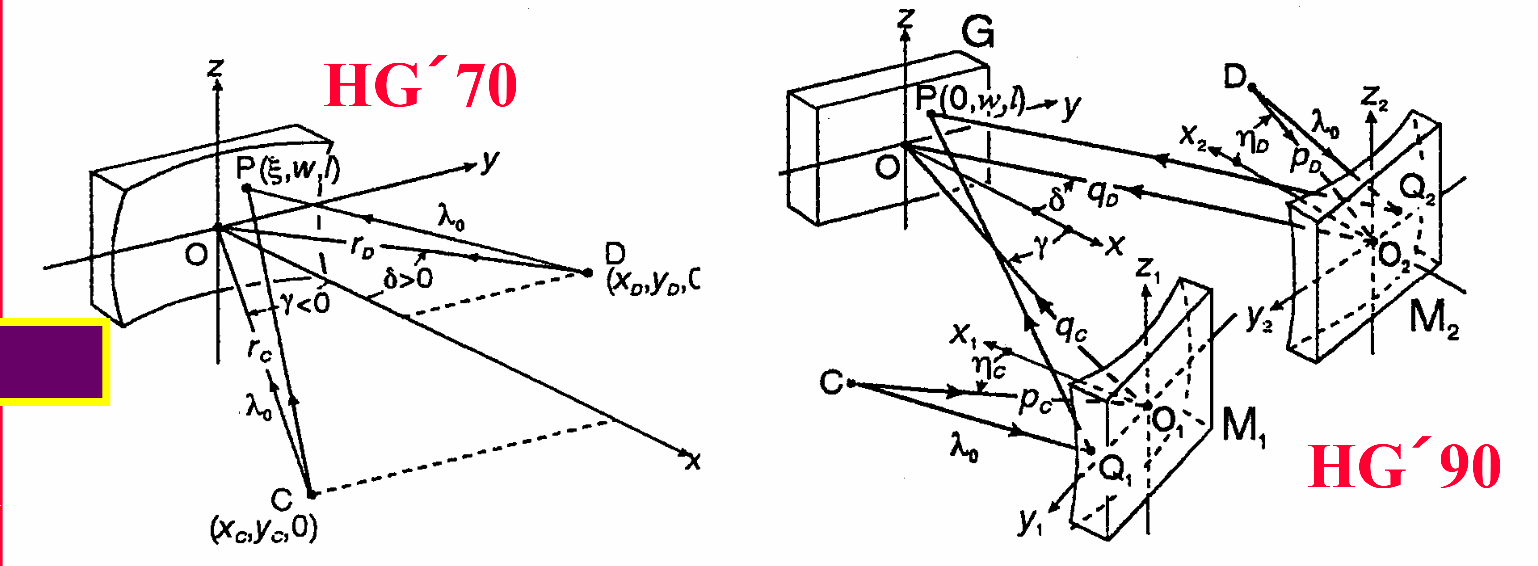

Namioka and Koike, Appl. Opt., **34**, 2180 (1995)

$$n_{20} = T_C - T_D, \quad n_{02} = S_C - S_D$$

$$n_{30} = \frac{T_C \sin\gamma}{r_C} - \frac{T_D \sin\delta}{r_D}, \quad n_{12} = \frac{S_C \sin\gamma}{r_C} - \frac{S_D \sin\delta}{r_D}$$

$$n_{40} = \frac{4T_C \sin^2\gamma}{r_C{}^2} - \frac{4T_D \sin^2\delta}{r_D{}^2} - \frac{T_C{}^2}{r_C} + \frac{T_D{}^2}{r_D} + \frac{S_C - S_D}{R^2}$$

.....

$$T_C = \frac{\cos^2\gamma}{r_C} - \frac{\cos\gamma}{R}, \quad T_D = \frac{\cos^2\delta}{r_D} - \frac{\cos\delta}{R}$$

$$S_C = \frac{1}{r_C} - \frac{\cos\gamma}{R}, \quad S_D = \frac{1}{r_D} - \frac{\cos\delta}{R}$$

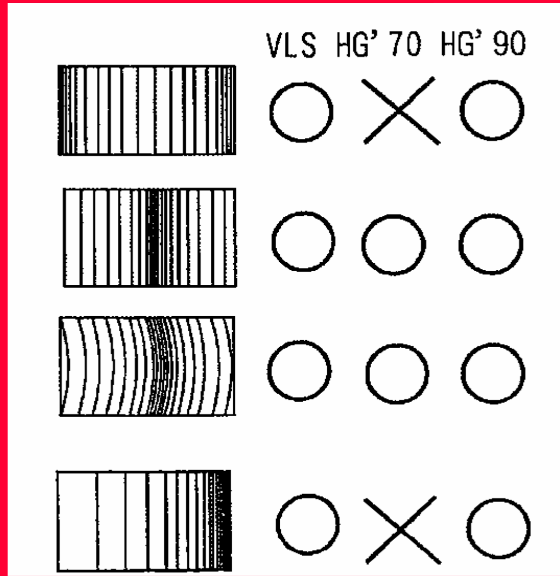

Monochromators in the VUV-SX region for SR use (1)

Normal incidence monochromators

M. Koike, "Normal incidence monochromators and spectrometers" in J.A.R. Samson and D.L. Ederer Eds., "Vacuum Ultraviolet Spectroscopy II in Experimental Methods in Physical Sciences" Vol. 32, (Academic Press, New York, 1998, Chapter 1, pp. 1-20 review

(A) Seya-Namioka type monochromator

(B) Pseudo Rowland mount monochromator

K. Ito, Y. Morioka, M. Ukai, N. Kouchi, Y. Hatano and T. Hayaishi, RSI, **66**, 2119 (1995)

(C) Eagle type monochromator

1) 6.65-m Eagle at BL-12B of the Photon Factory

K. Ito, T. Namioka, Y. Morioka, T. Sasaki, H. Noda, K. Goto, T. Katayama and M. Koike, Appl. Opt., **25**, 837-847 (1986)
K. Ito and T. Namioka, Rev. Sci. Instr., **60**, 1573-1578 (1989)
K. Ito, K. Maeda, Y. Morioka and T. Namioka, Appl. Opt., **28**, 1813-1817 (1989)

2) undulator based 6.65-m Eagle at BL9.02 of ALS

M. Koike, P. Heimann, A. Kung, T. Namioka, R. DiGennaro, B. Gee and N. Yu, NIM, **A347**, 282 (1994)
A.G. Suits, P. Heimann, X. Yang, M. Evans, C.W. Hsu, K. Lu, Y.T. Lee and A.H. Kung, RSI, **66**, 4841 (1995)
D.A. Mossessian, P. Heimann, E. Gullikson, R.K. Kaza, J. Chin and J. Arke, NIM, **A347**, 244 (1994)

3) 6.65-m Eagle with varibale polarization undulator at SU5 of LURE

L. Nahon, B. Lagarde, F. Polack, C. Alcaraz, O. Dutuit, M. Vervloet and K. Ito, NIM, **A404**, 418-429 (1998)
K. Ito, B. Lagarde, F. Polack, C. Alcaraz and L. Nahon, J. Synchrotron Rad., **5**, 839-841 (1998)
L. Nahon, C. Alcaraz, J-J. Marlats, B. Lagarde, F. Polack, R. Thissen, D. Lepere and K. Ito, RSI, **72**, 1320 (2001)

Seya-Namioka monochromator (1)

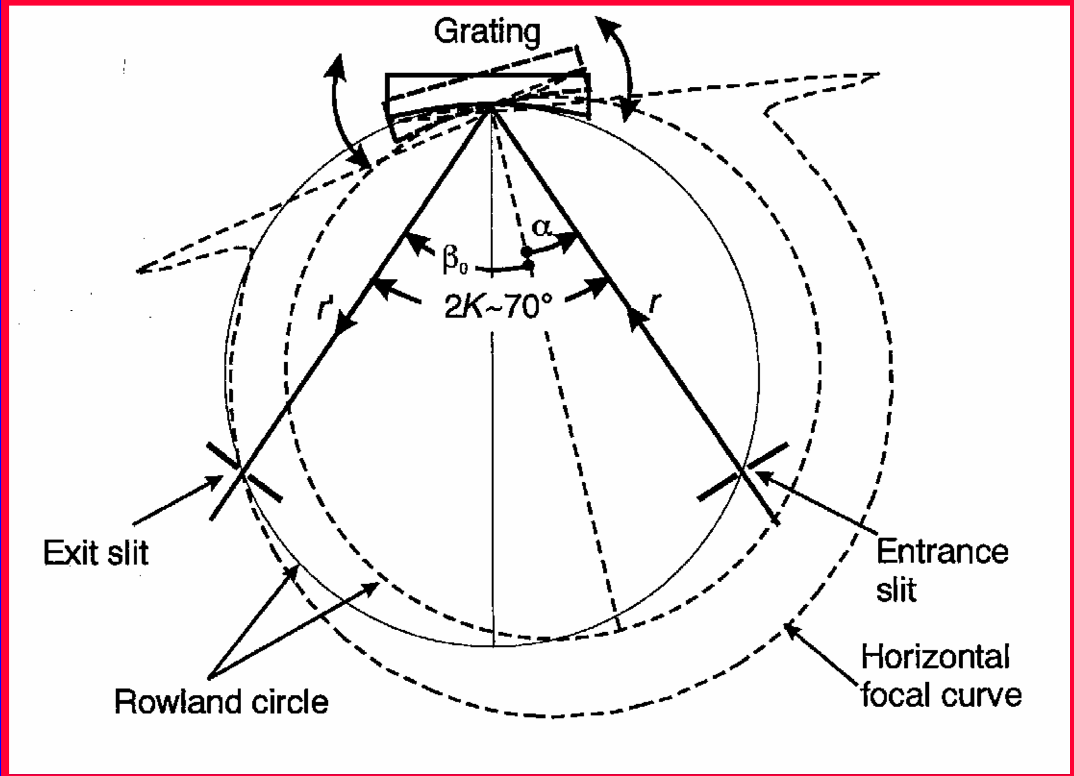

$$I_{200} = \int_{\theta_1}^{\theta_2} F_{200}{}^2 d\theta$$

$$\frac{\partial I_{200}}{\partial r} = 0, \quad \frac{\partial I_{200}}{\partial r'} = 0, \quad \frac{\partial I_{200}}{\partial K} = 0$$

→

R/r=1.220527
R/r’=1.216931
2K=69.44°

Seya-Namioka monochromator (2)

1000 rays, generated from the entrance slit 10mm long, hitting the 1800-grooves/mm grating with 100(W)×60(H) mm² : from Koike's review

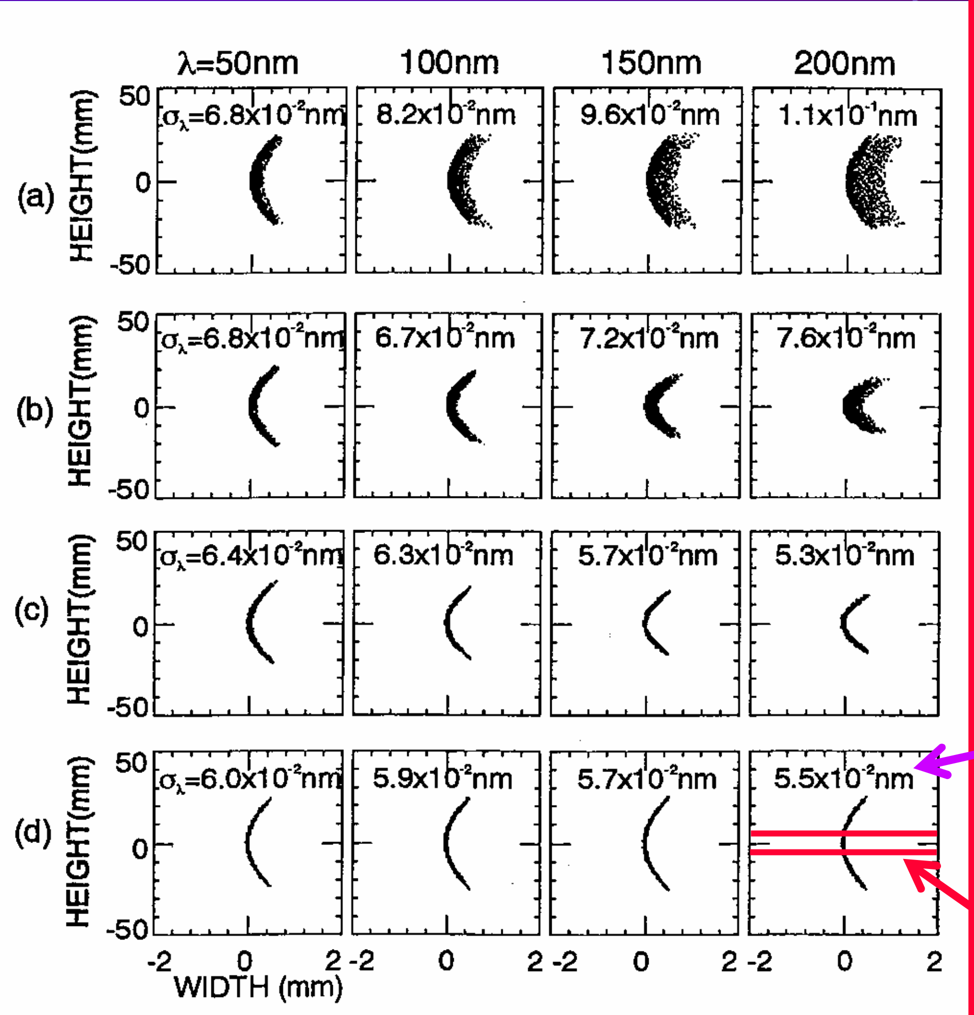

conventional grating

holographic grating recorded with a spherical wave front

holographic grating recorded with an aspherical wave front

E/ΔE≈3600

VLS grating with straight grooves

E/ΔE≈3×10⁴
Through put: 23%

Pseudo Rowland mount monochromator

Robin-Romand mount

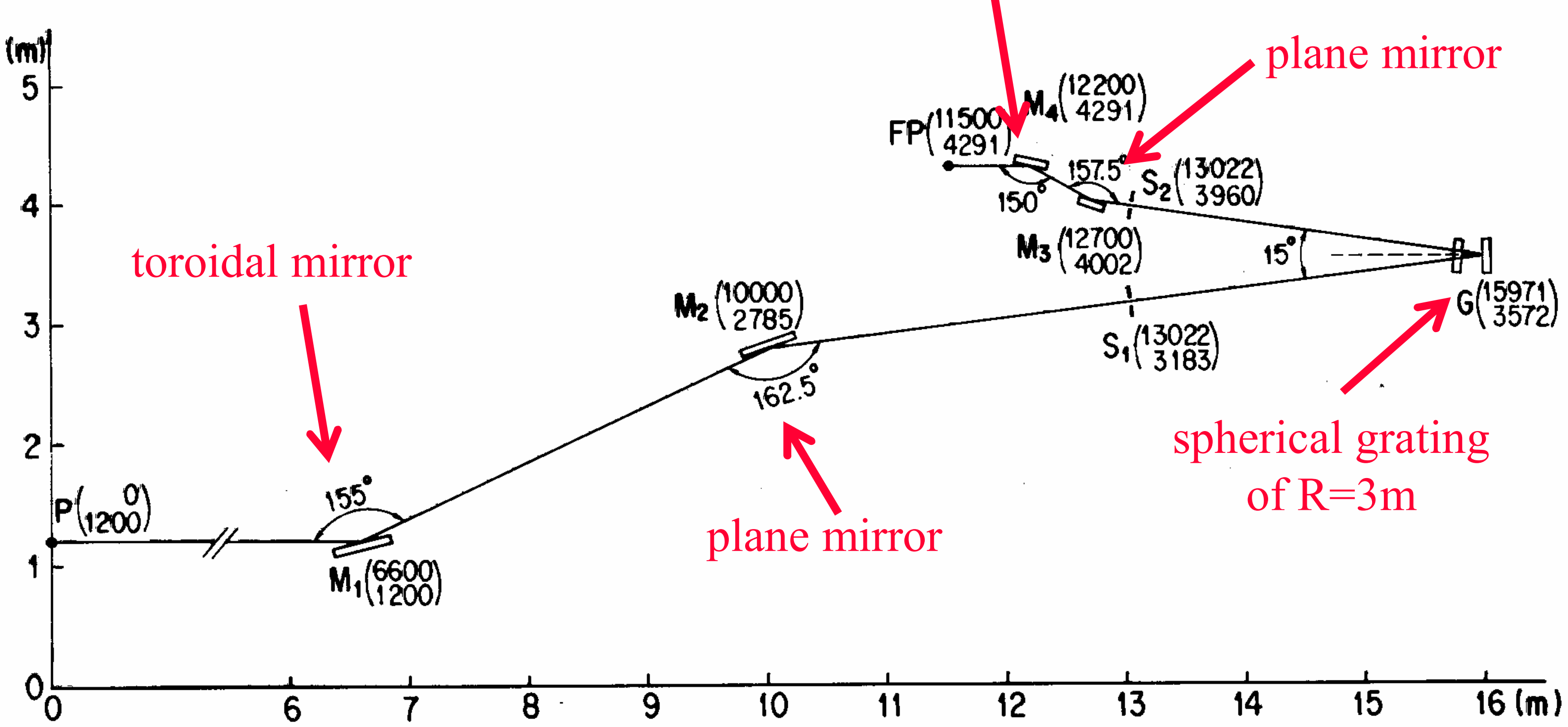

K. Ito, Y. Morioka, M. Ukai, N. Kouchi, Y. Hatano and T. Hayaishi, RSI, **66**, 2119 (199

Pseudo Rowland mount monochromator

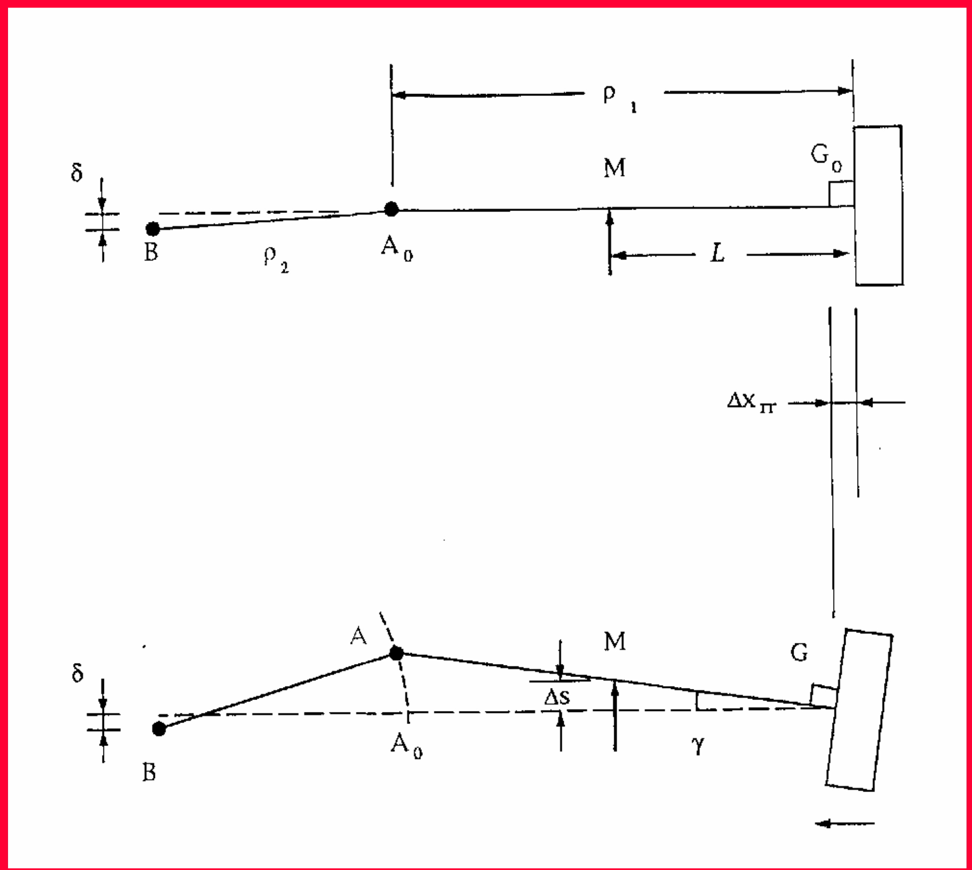

$$F_{20} = \frac{\cos^2\alpha}{r} - \frac{\cos\alpha}{R} + \frac{\cos^2\beta}{r'} - \frac{\cos\beta}{R}$$

Δ_{th} is calculated by $F_{20}=0$.

ρ_2 and δ are chosen so that

$$\sum_{\lambda=30\,nm}^{200\,nm} (\Delta_{rr} - \Delta_{th})^2 \quad \text{is minimized.}$$

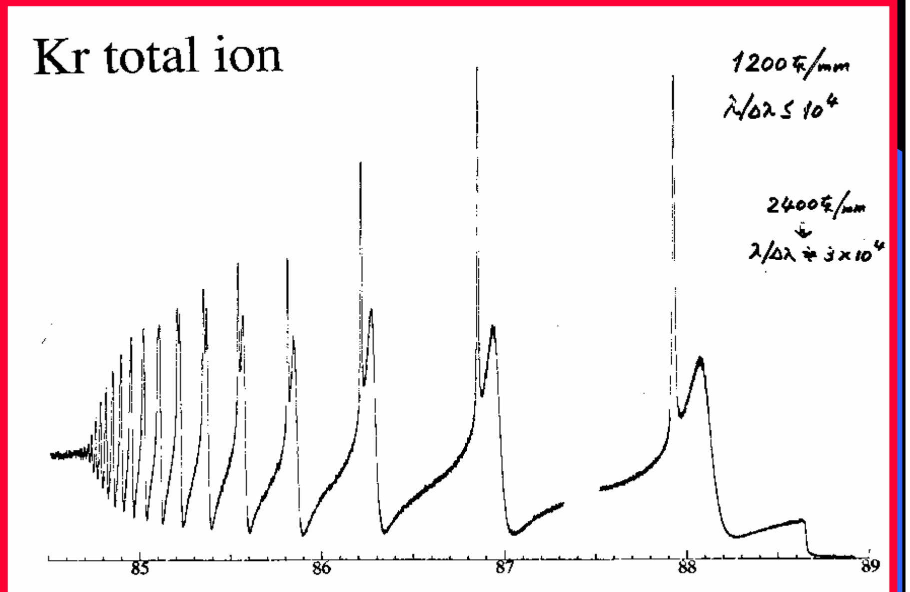

K. Ito, Y. Morioka, M. Ukai, N. Kouchi,
Y. Hatano and T. Hayaishi, RSI, **66**, 2119 (1995)

With a 2400-*l*/*mm* grating,
$E/\Delta E \leq 3\times10^4$ can be attained.

Off-plane Eagle (1)

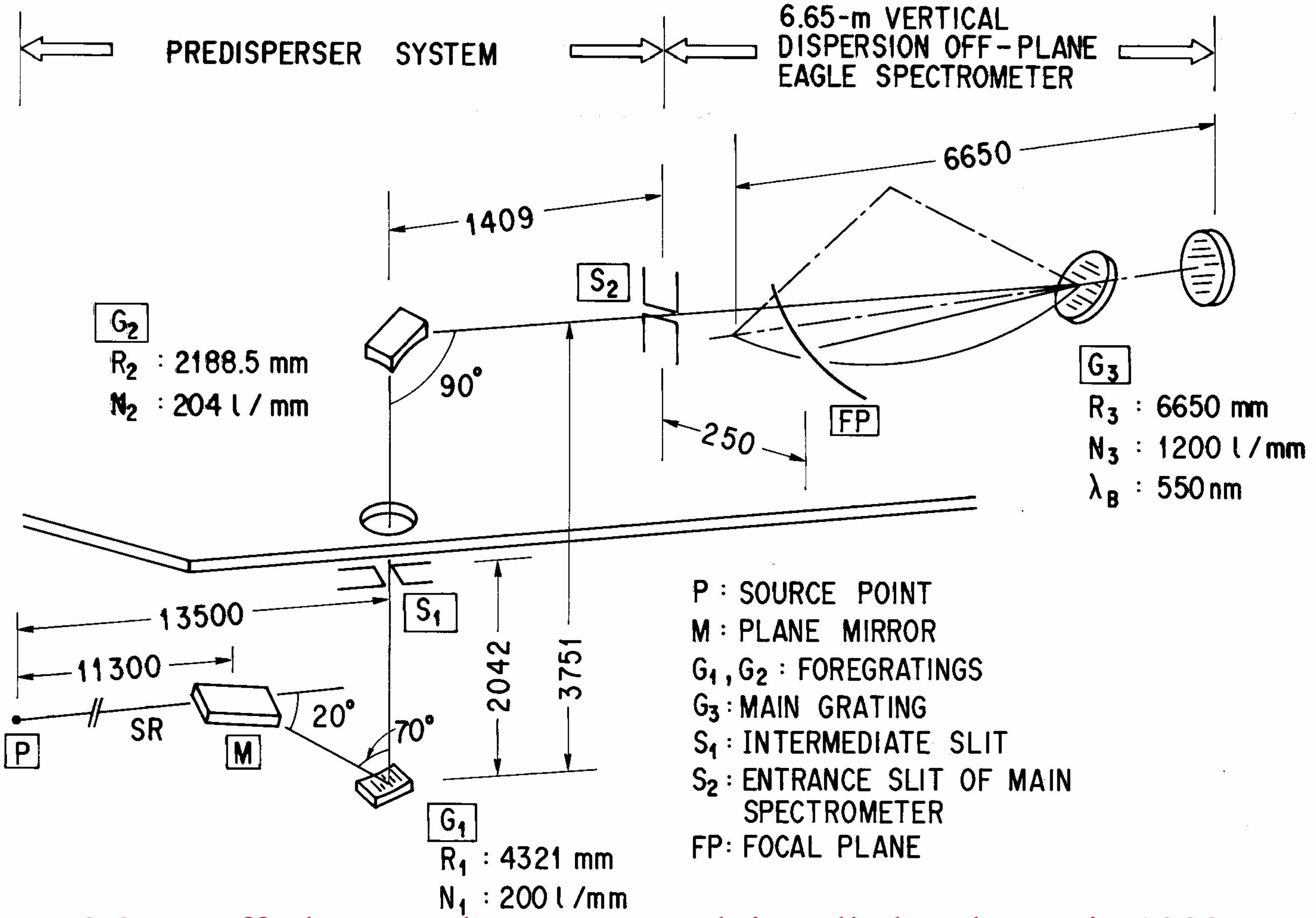

6.65-m off-plane Eagle spectrograph installed at the PF in 1983

Off-plane Eagle (2)

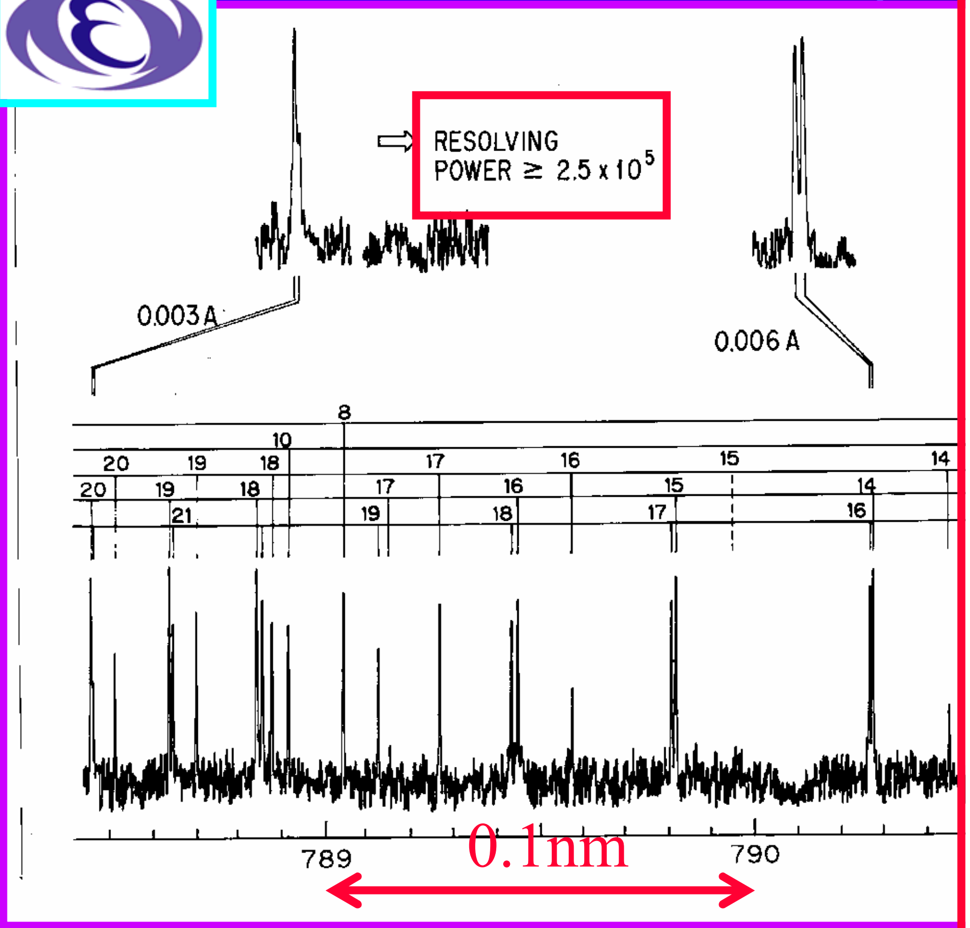

Photographic

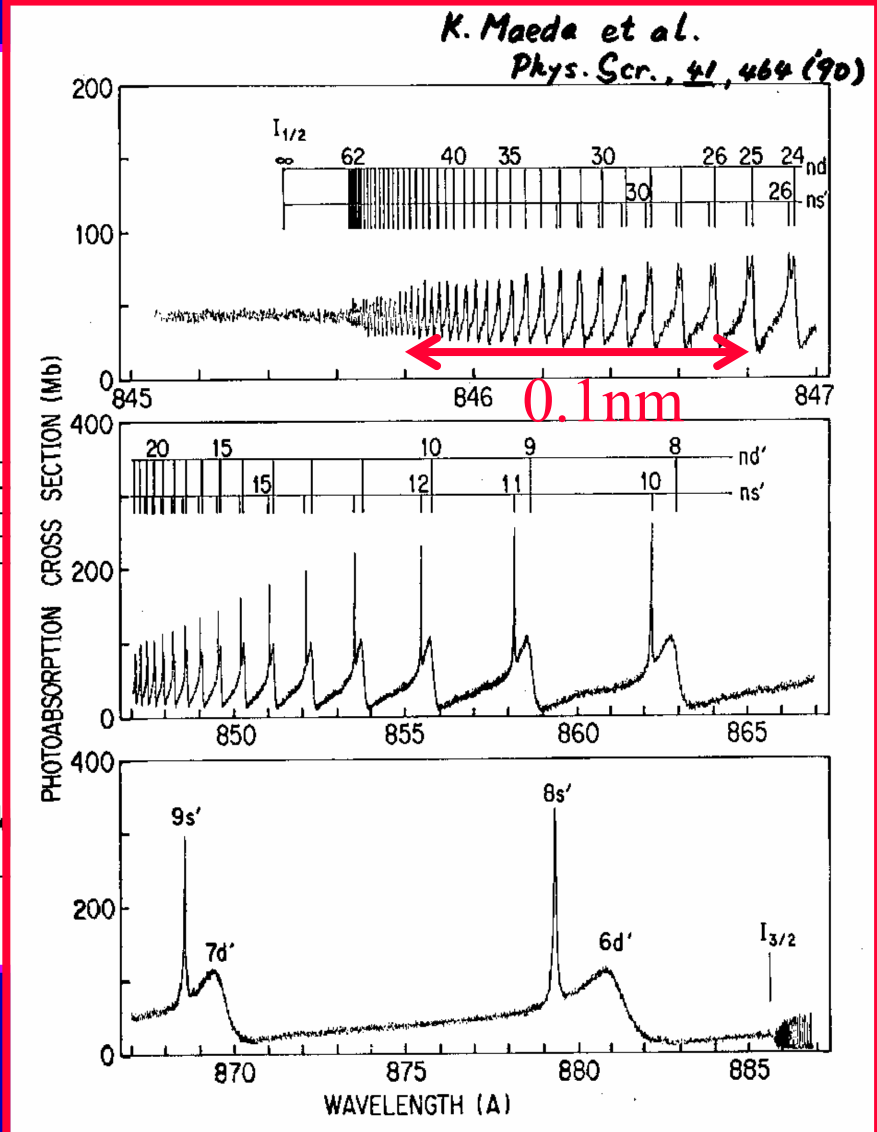

Photoelectric

Off-plane Eagle (3)

Molecular beams, lasers, and undulator radiation

Molecular spectroscopy, 5 to 30 eV (400 to 2500Å)

Photodissociation ALS

Absorbed power density of M_1 and M_2 are 10.4 and 7.6 W/cm^2.

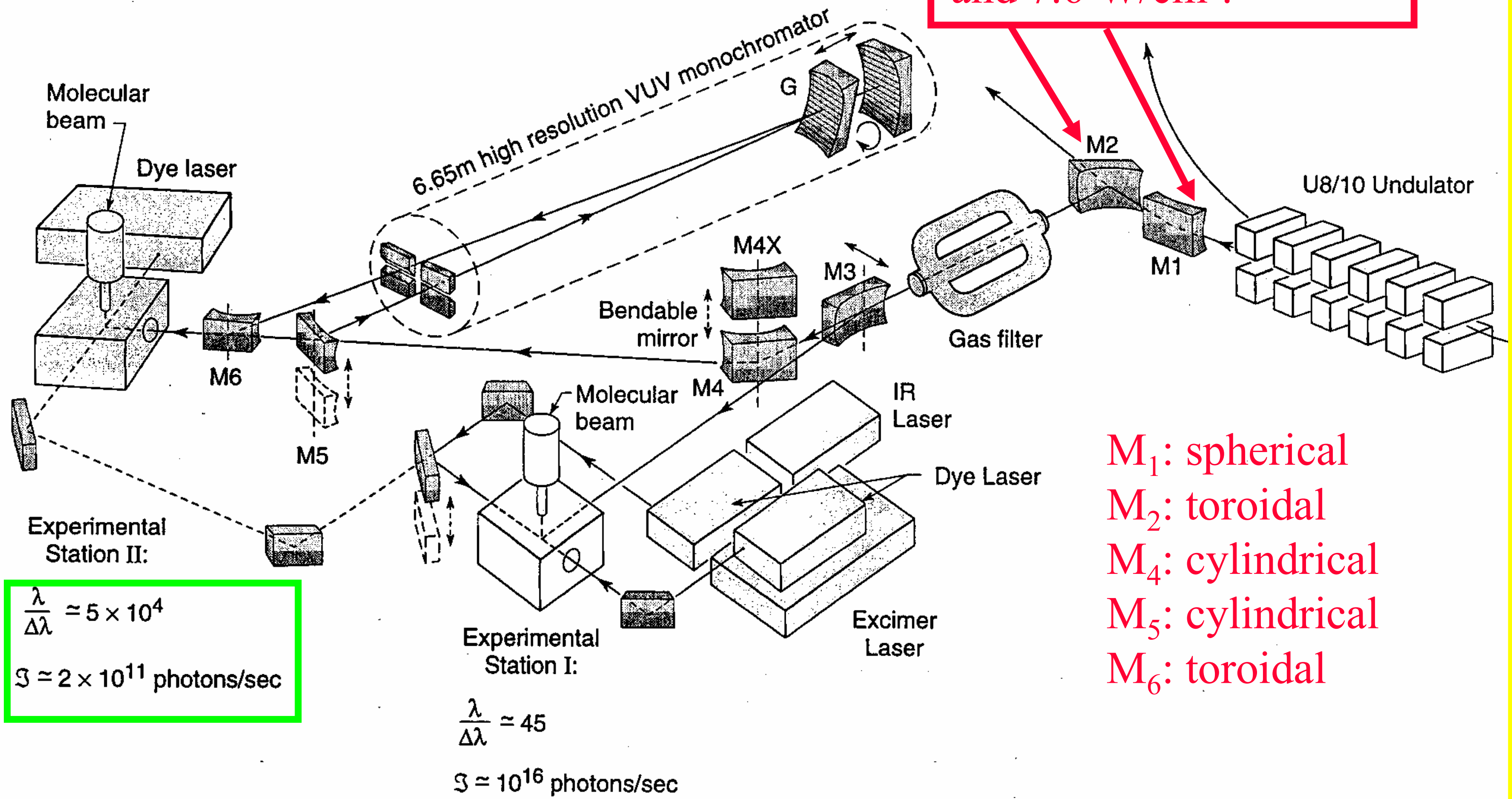

M_1: spherical
M_2: toroidal
M_4: cylindrical
M_5: cylindrical
M_6: toroidal

Koike, Heimann, Kung, Namioka, DiGennaro, Gee and Yu, NIM, **A347**, 282 (1994)

Off-plane Eagle (4)

VUV high-resolution b[…]
with variable polarizati[…]
of SACO (LURE)

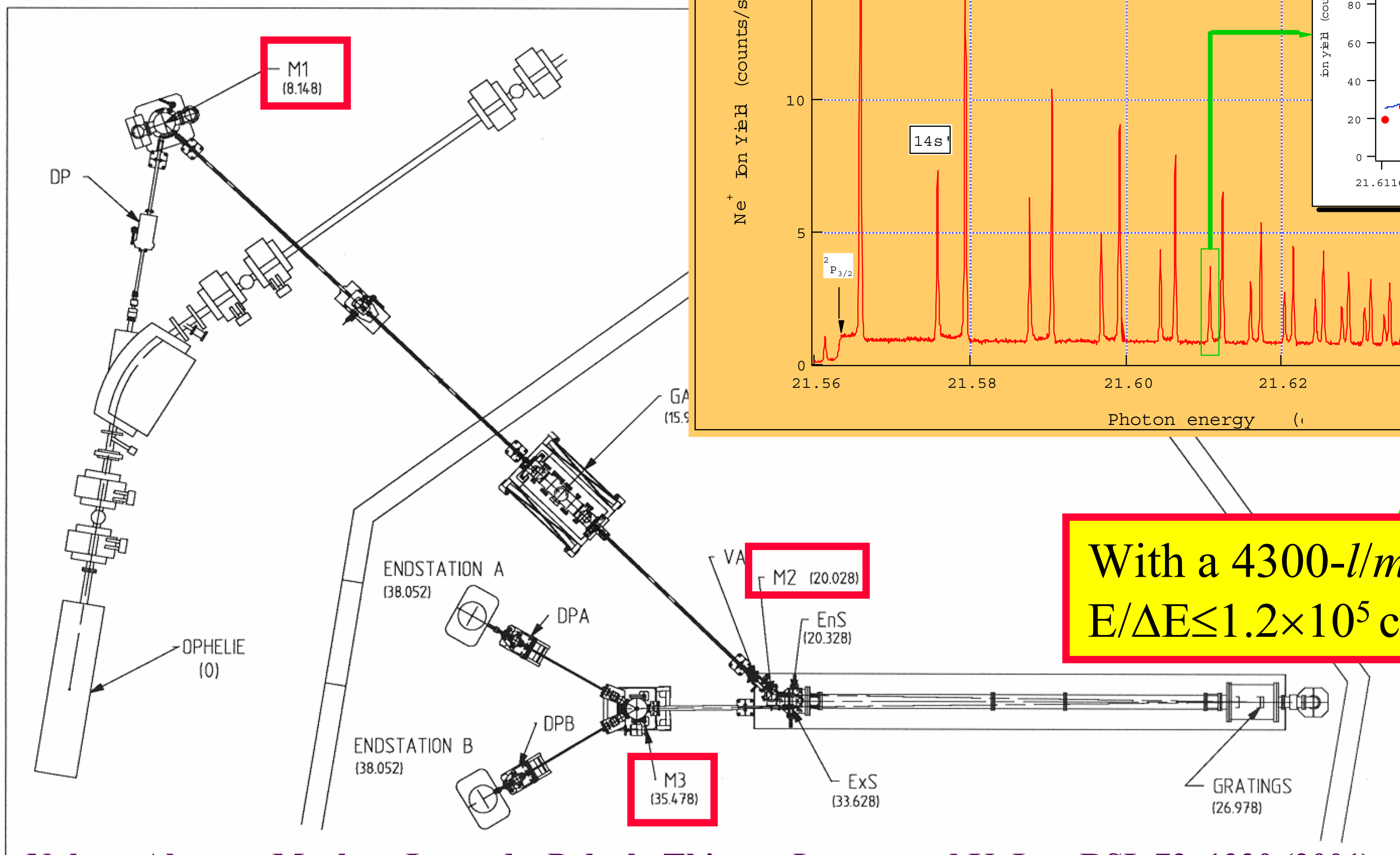

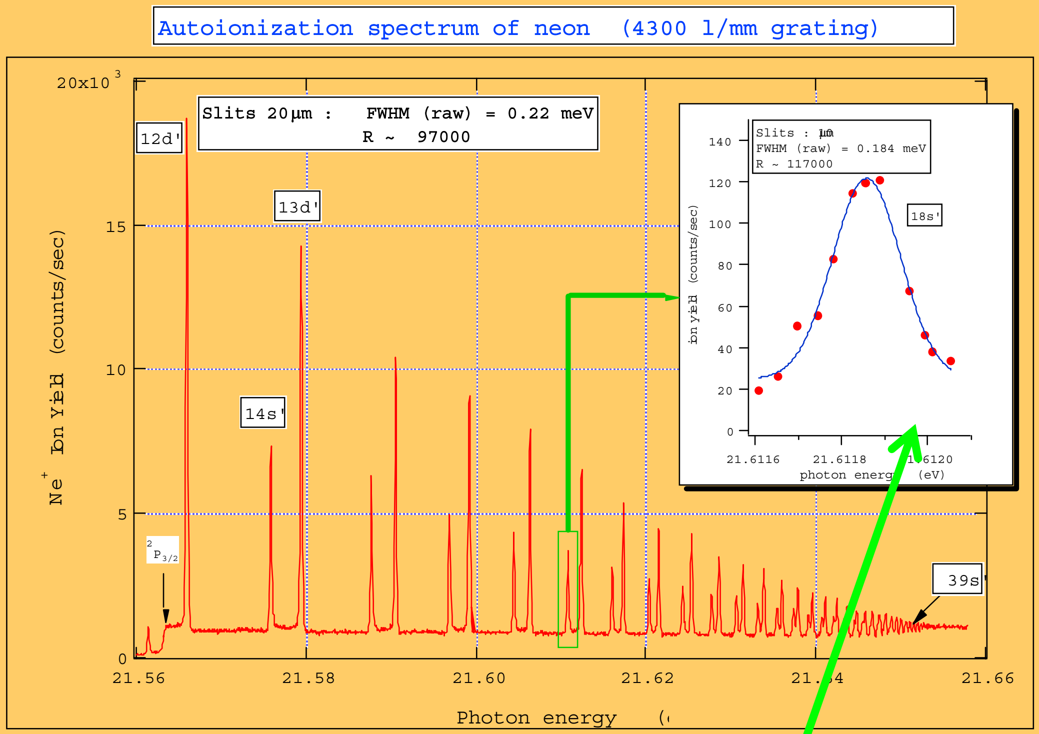

With a 4300-*l*/*mm* grating, $E/\Delta E \leq 1.2\times10^5$ can be attained.

Nahon, Alcaraz, Marlats, Lagarde, Polack, Thissen, Lepere and K. Ito, RSI, 72, 1320 (2001)

Monochromators in the VUV-SX region for SR use (2)

Grazing incidence monochromators

(A) Spherical grating monochromator (SGM) or Dragon
C.T. Chen, NIM, **A256**, 595 (1987); C.T. Chen and F. Sette, RSI, **60**, 1616 (1989).

(B) SX700 (PGM, elliptical mirror) and modified SX700
H. Petersen, Opt. Com., **40**, 402 (1982); H.A. Padmore, RSI, **60**, 1608 (1989);
H. Petersen et al., RSI, **66**, 1777 (1995).

(C) Monk-Gillieson type monochromator
M. Hettrick et al., Appl. Opt., **27**, 200 (1988); M. Koike and T. Namioka, RSI, **66**, 2114 (1995).

(D) Harada type monochromator (PGM)
T. Harada, M. Itou and T. Kita, Proc. SPIE, **503**, 114 (1984); M. Itou, T. Harada and T. Kita, Appl. Opt., **28**, 146 (1989).

(E) Grasshopper monochromator: Rowland mount
F.C. Brown et al., NIM, **152**, 73 (1978); F. Senf et al., RSI, **63**, 1326 (1992).

SGM at the BL-16B of the PF (1)

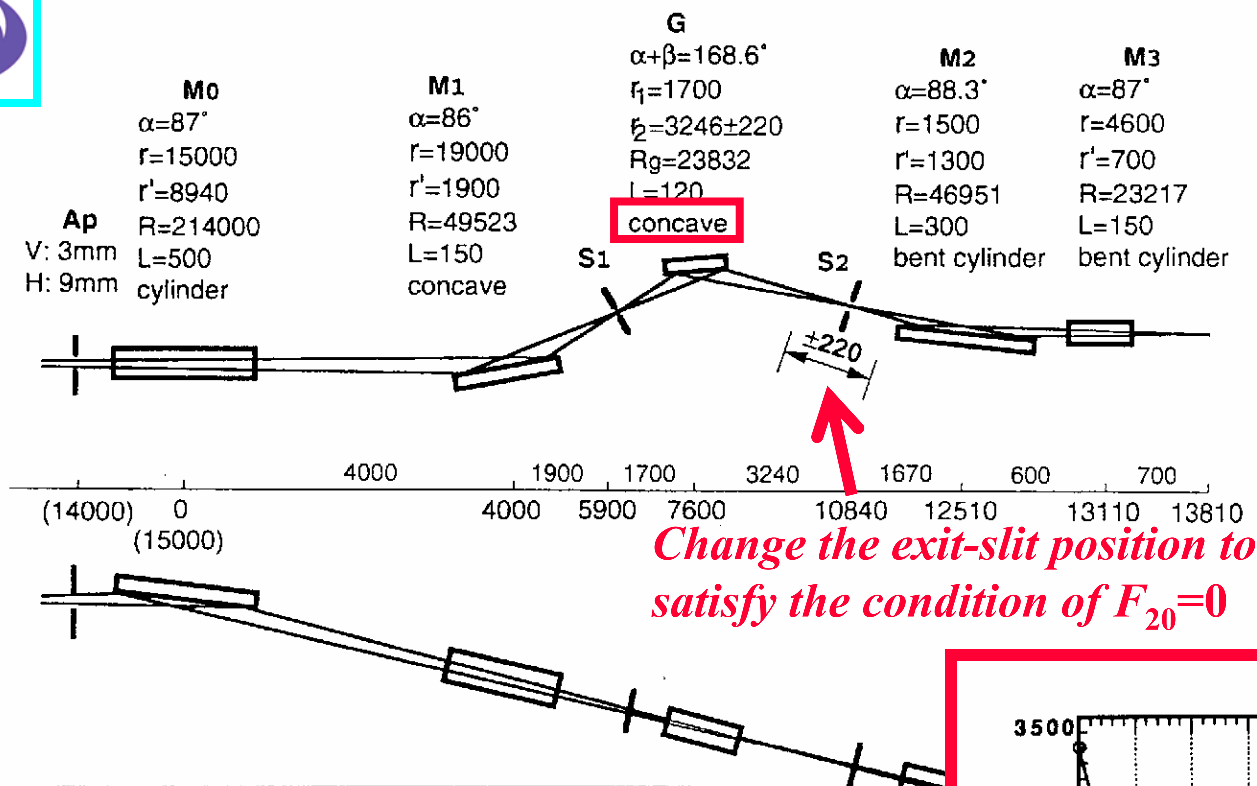

Change the exit-slit position to satisfy the condition of F_{20}=0

Parameters of the source		
Ring energy and current:	E_e=2.5GeV	I_e=300mA
Beam emittance:	σ_x=0.78mm	σ_y=0.11mm
	σ_x'=0.16mrad	σ_y'=0.022mrad
Undulator:	λ_u=12cm	N=26

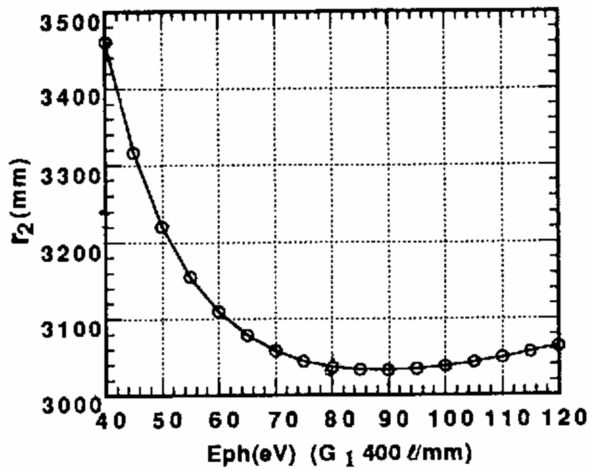

Shigemasa et al., JSR, **5**, 772 (1998)

SGM at the BL-16B of the PF (2)

Theoretical estimation for resolving power

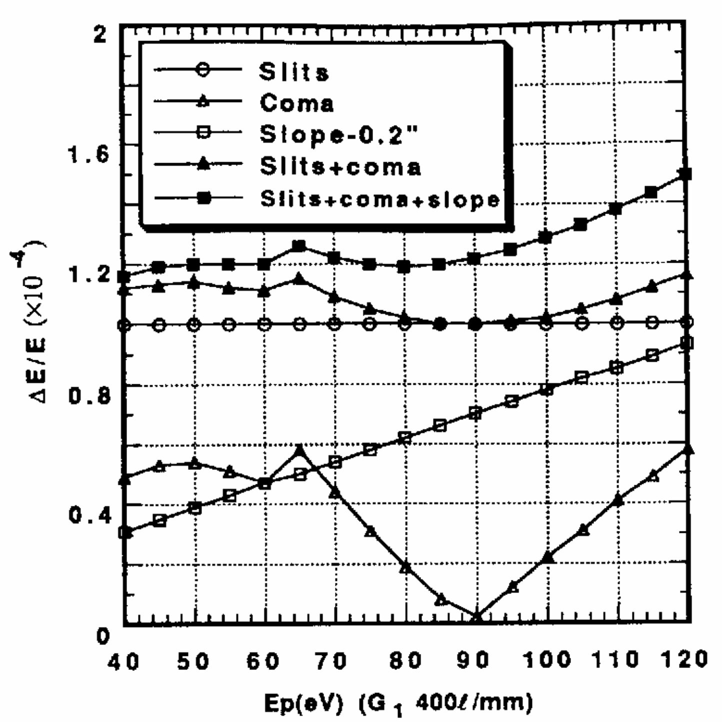

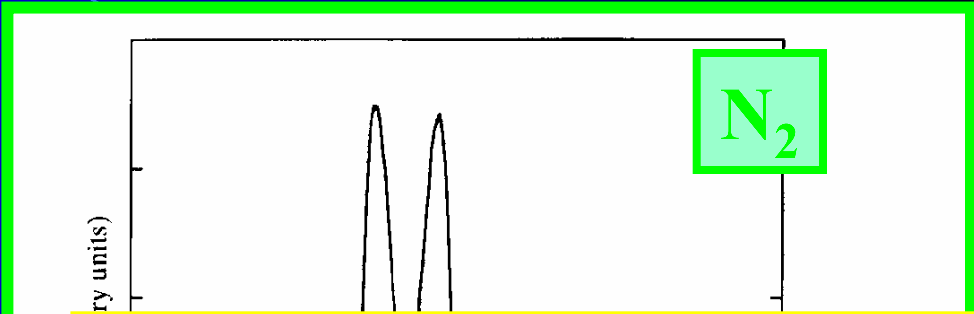

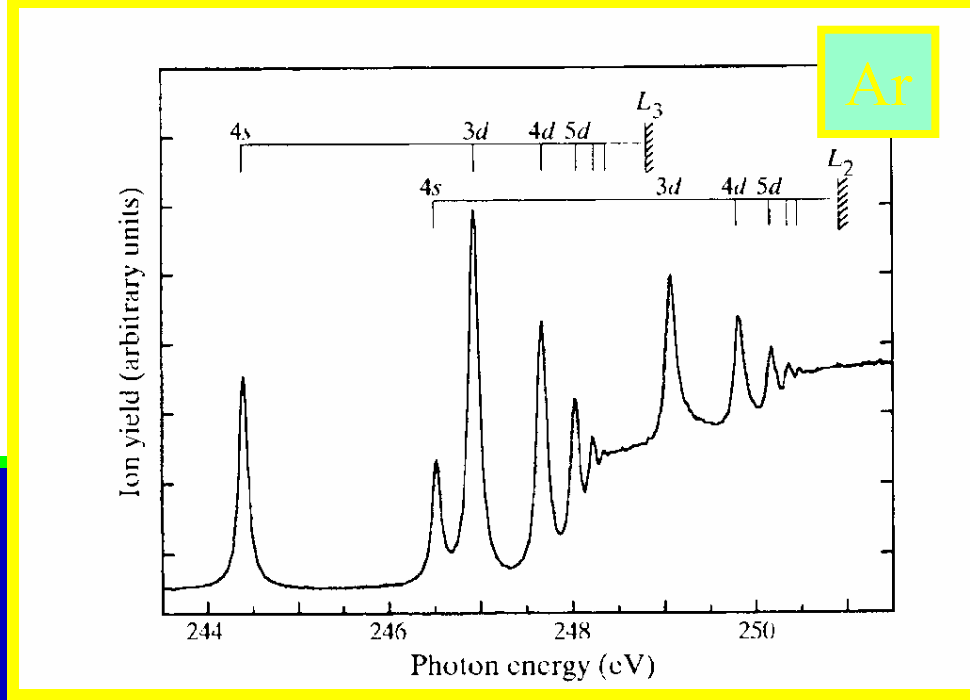

Shigemasa et al., JSR, **5**, 772 (1998)

SX-700

H. Petersen, Opt. Com., **40**, 402 (1982)

$$F_{20} = \frac{\cos^2\alpha}{r} - \frac{\cos\alpha}{R} + \frac{\cos^2\beta}{r'} - \frac{\cos\beta}{R}$$

F_{20}=0 with $R=\infty$

$$r = -r'\frac{\cos^2\beta}{\cos^2\alpha}\left(= -r'C\right)$$

C=2.25 high grating efficiency

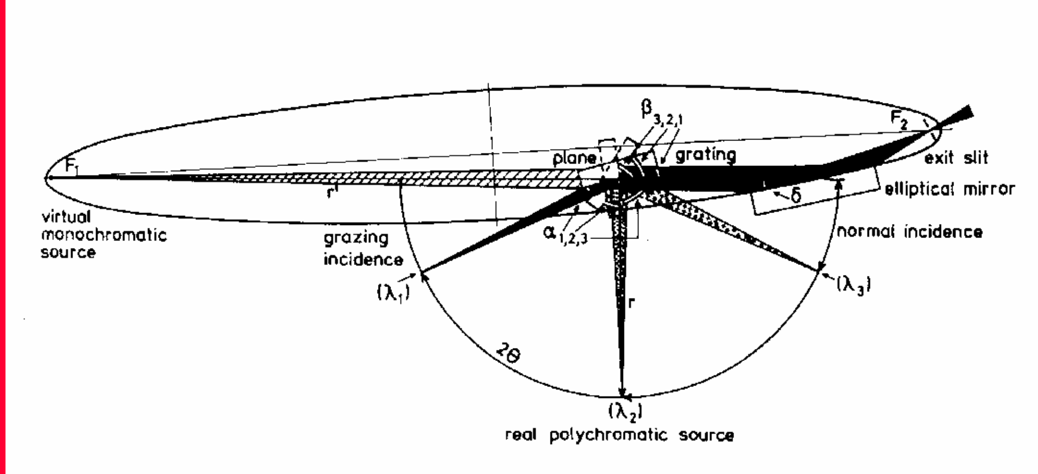

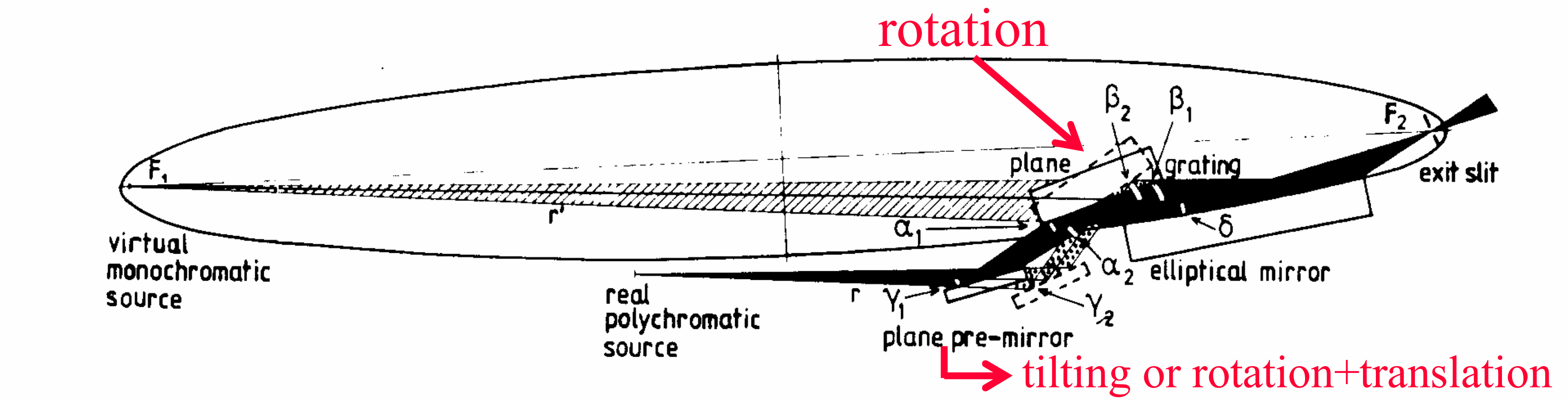

Modified SX-700 on-blaze type monochromator

Padmore, RSI, **60**, 1608 (1989); Petersen et al., RSI, **66**, 1777 (1995).

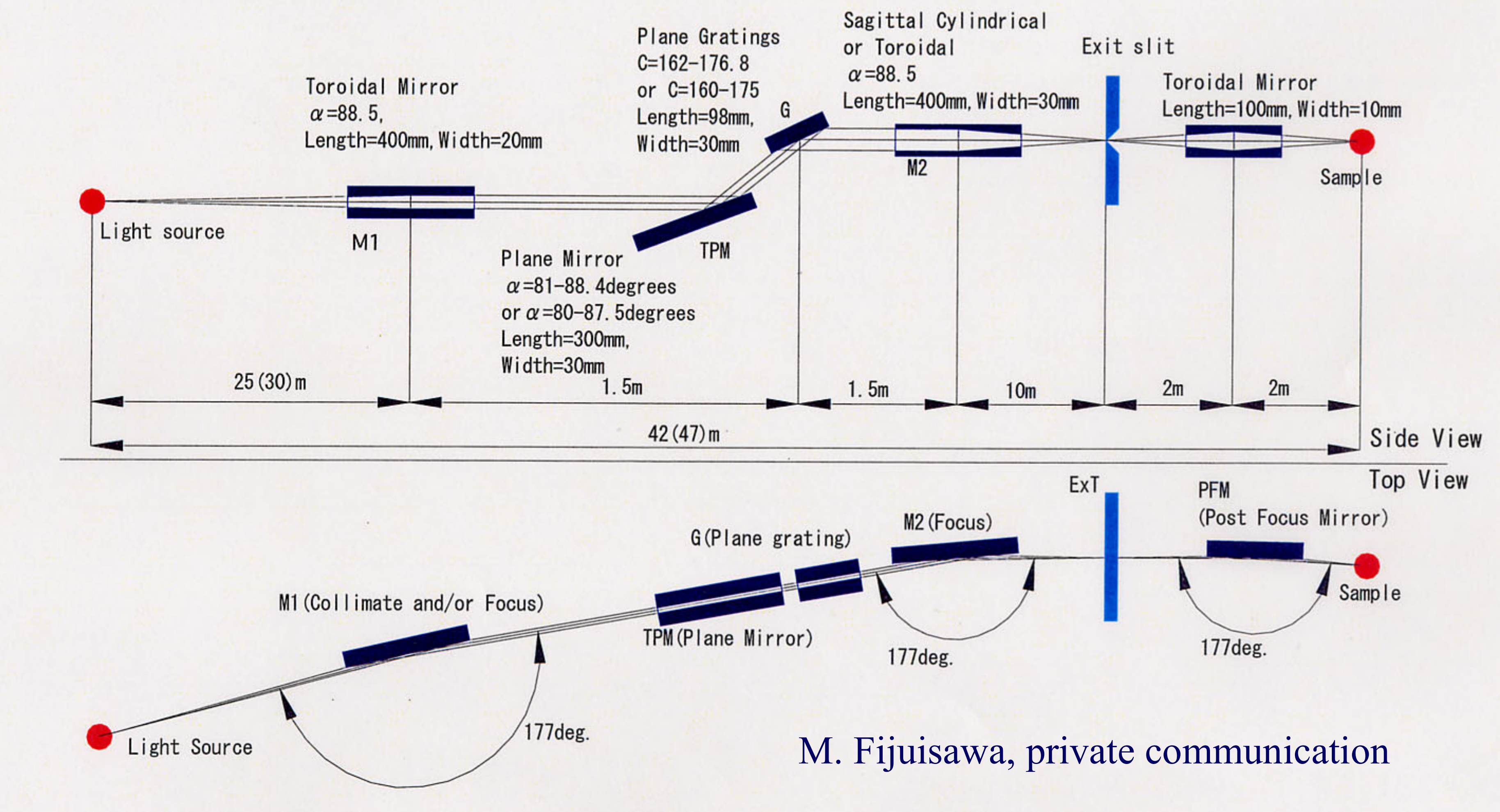

M. Fijuisawa, private communication

Monk-Gillieson type monochromator

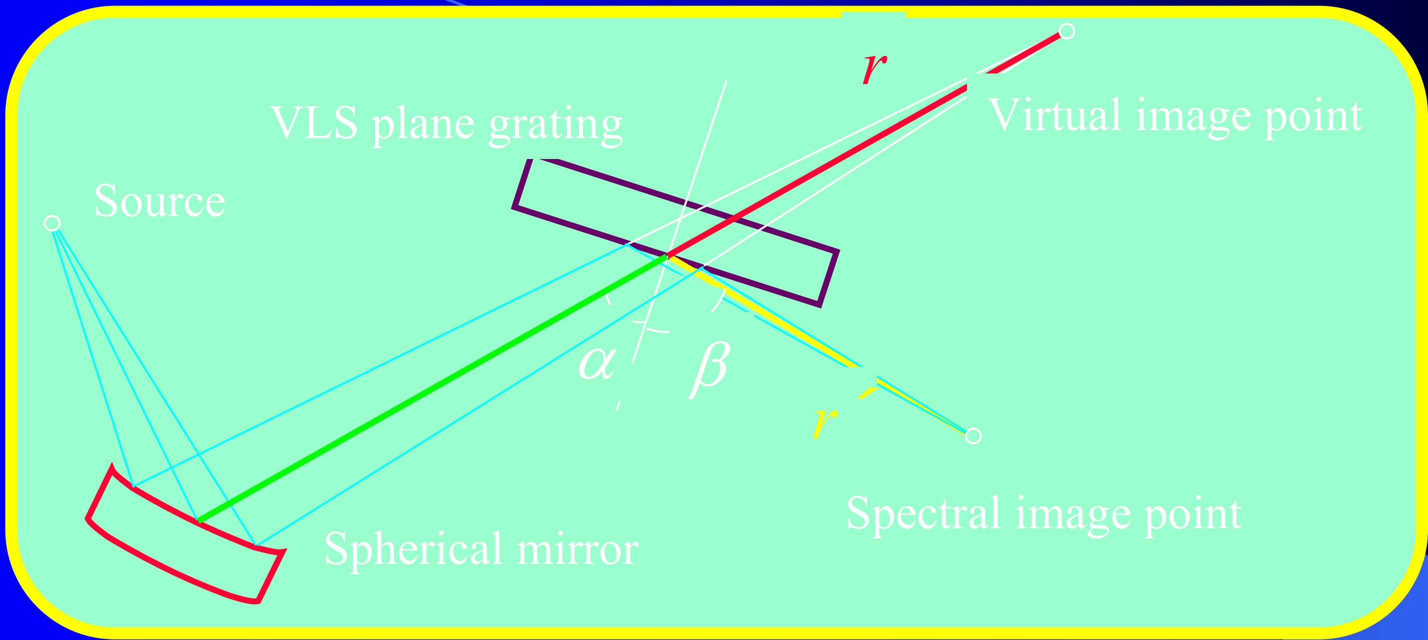

Defocus term : $$F_{20} = \frac{\cos^2\alpha}{r} - \frac{\cos\alpha}{R} + \frac{\cos^2\beta}{r'} - \frac{\cos\beta}{R} + \frac{\Gamma m n_{20}\lambda}{\sigma}$$

$R = \infty$, $\Gamma = 1$ and $m = +1$

$$F_{20} = \frac{\cos^2\alpha}{r} + \frac{\cos^2\beta}{r'} + \frac{n_{20}\lambda}{\sigma}$$

F_{30} and F_{40} can be taken into account, however, it is difficult to control.

Hettrick et al., Appl. Opt., **27**, 200 (1988); Koike and Namioka, RSI, **66**, 2114 (1995).

BL-11A (1)

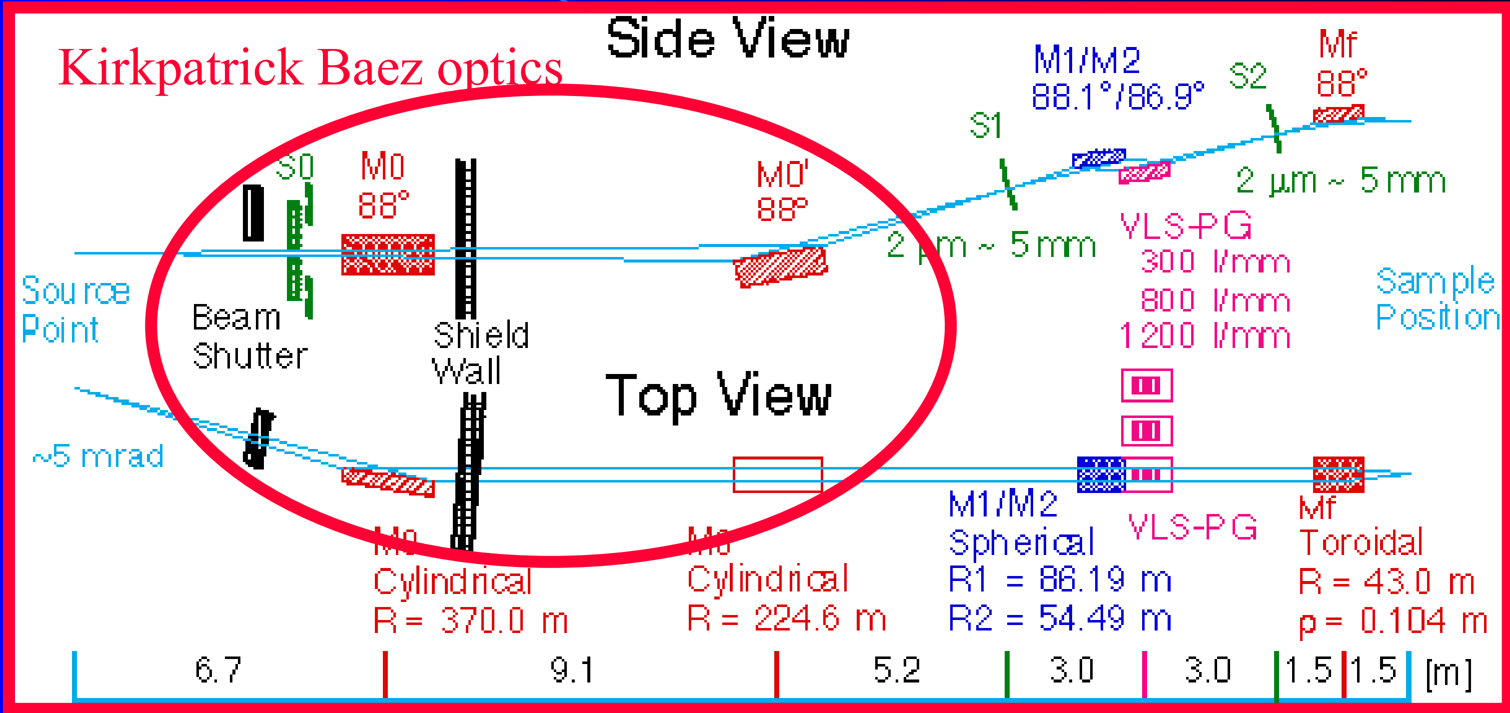

$r = -r'$ F_{20}=0 at zeroth order and 500 eV

↓

facilitate the optical adjustment

Amemiya, Kitajima, Ohota and Ito, JSR, **3**, 282 (1996); Kitajima, Amemiya, Yonamot
Ohta, Kikuchi, Kosuge, Toyoshima and Ito, JSR, **5**, 729 (1998); Kitajima, Yonamoto,
Amemiya, Tsukabayashi, Ohta and Ito, JESRP, **101-103**, 927 (1999).

BL-11A (2) transmission

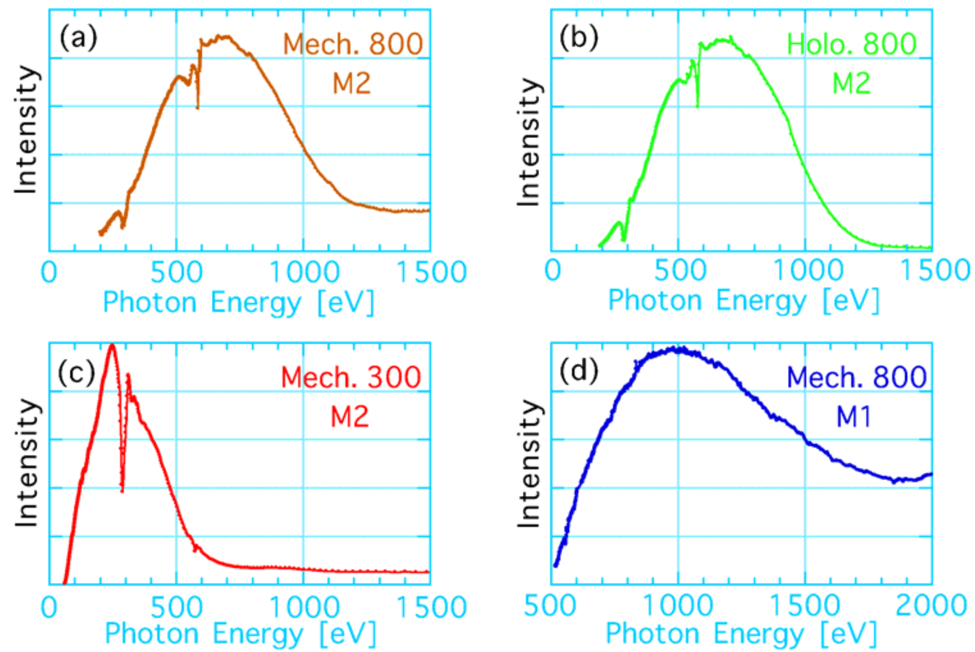

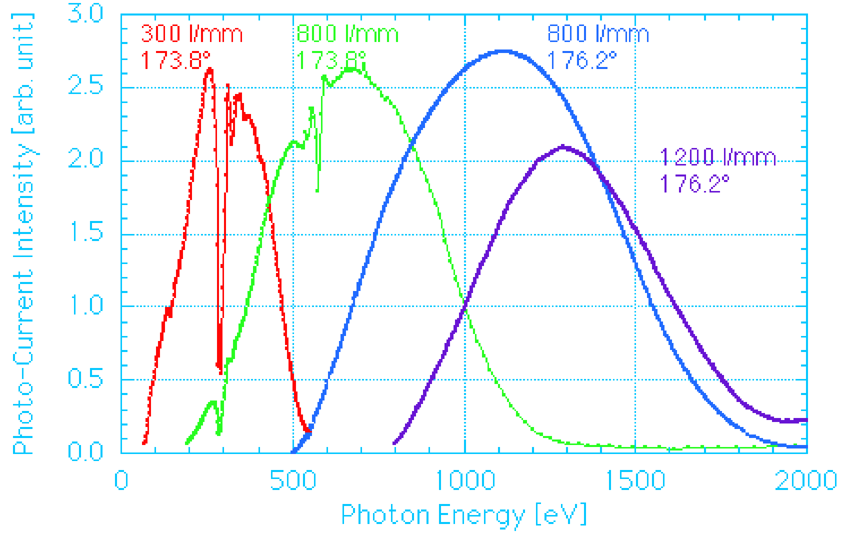

BL-11A (3) N_2 absorption

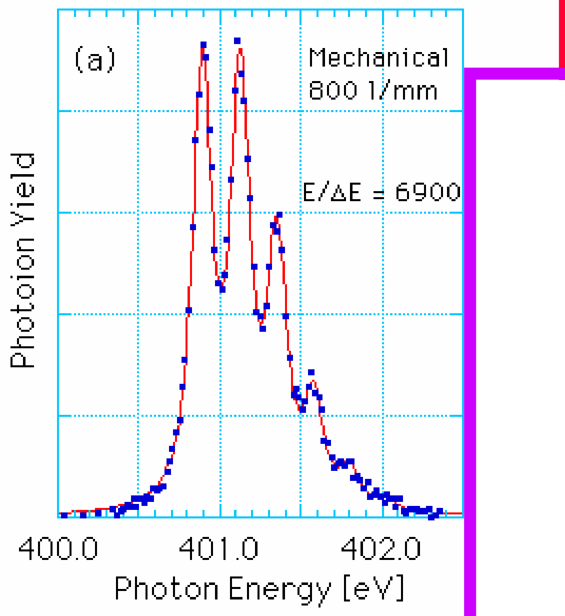

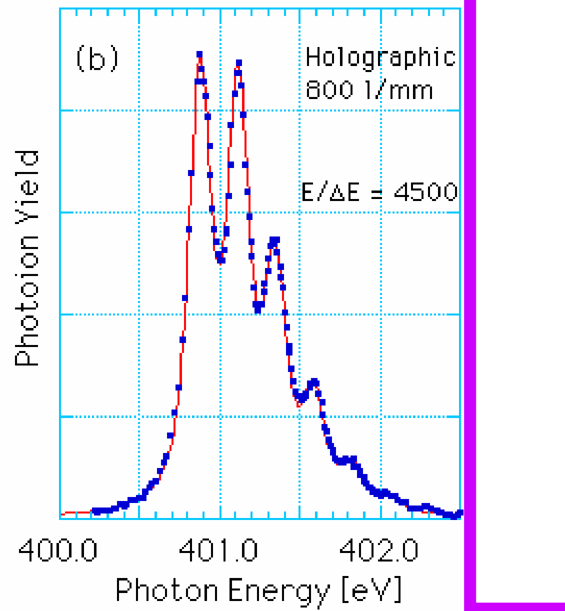

slit widths vs. resolution/flux

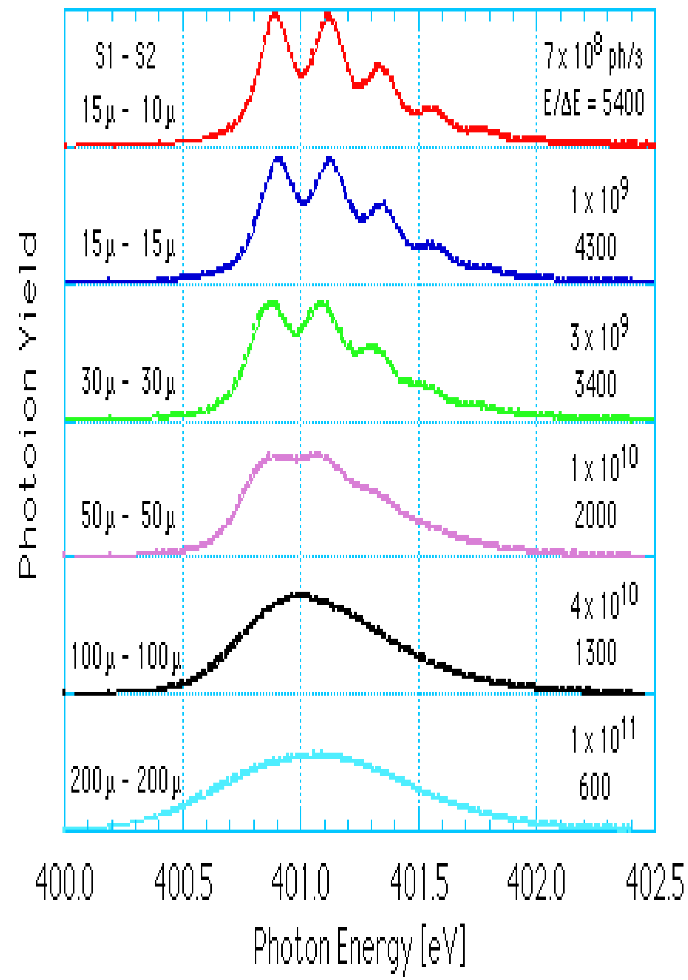

Other important points in the construction of VUV-SX beamlines (1)

Hardware design

Wavelength-scanning mechanism in monochromator: the precision of grating rotation is in the order of 1/100 sec.
In-situ adjustment of optical elements, such as rotations and translation.
Enclosing the important parts in a temperature controlled booth.

Isolation of optical elements

Optical elements or optical benches are well isolated from mechanical vibrations caused by ventilators, mechanical pumps, and so on. An ideal beamline is installed on a massive concrete base.

Other important points in the construction of VUV-SX beamlines (2)

Installing beamlines

Anticipate how to align beamlines in its design stage.
Convenient tools for beamline alignment: theodolites and auto-levels with a telescope and a laser

Optical alignment

VUV-SX photons are not visible!!!
Beam position monitors such as fluorescent screens, photodiodes, and wire monitors are needed.

Other important points in the construction of VUV-SX beamlines (3)

Heat load on optical elements

Cooling system

For VUV-SX beamlines, direct cooling is difficult! In-Ga alloy is used for better thermal contact between mirrors/gratings and their water cooled holders. Entrance slits are often required to be cooled.

Thermal distortion

Selecting materials with small value for α/κ as substrate of mirrors and gratings. SiC and Si are favored.

Simulation by ANSYS

Other important points in the construction of VUV-SX beamlines (4)

Specification of mirrors and gratings

Consult the makers about the micro roughness, slope error, and groove density, of optical elements, for which the beamline performance is strongly dependent.

Vacuum technology

Vacuum technology is well established to obtain 10^{-8} Pa (10^{-10} Torr).
Clean vacuum is obtained by oil-free primary pumps.
Contamination of optical elements.
cleaning with O_2 discharge and UV-lamp.

Other important points in the construction of VUV-SX beamlines (5)

Control systems of beamline

PC-base control system for the monochromator including the interface boards for stepping motors and encoders

Beam channel?

Beamline interlock system to protect the experimentalists from radiation hazards and to avoid vacuum problems

Characterization of beamlines

Photon flux, resolving power, purity of light,

Reproducibility of the wavelength scanning

Fluctuation of the beam position on the entrance slit

Other important points in the construction of VUV-SX beamlines (6)

Safety

Radiation safety

Gamma-ray stopper downstream of the first mirror, which might be installed inside a cage

Flammable and toxic gases

Gas duct with a gas detection system
Exhaust steam from rotary pumps